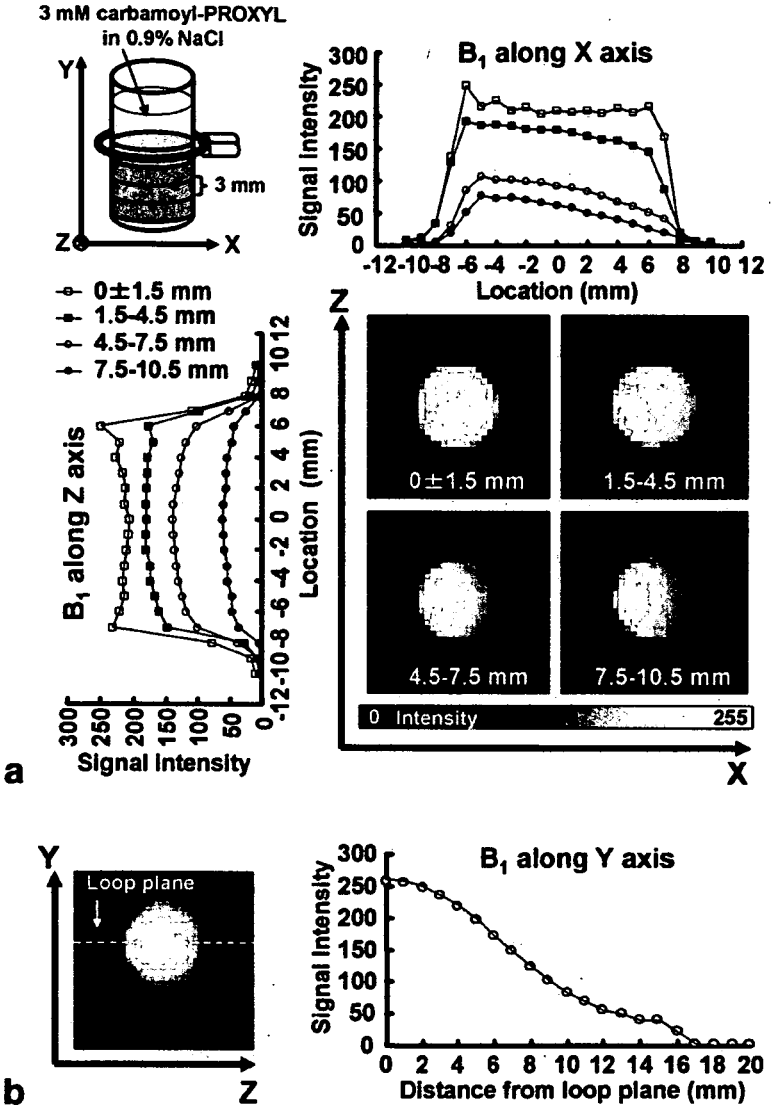

FIG. 3. **a:** Homogeneity of the OMRI signal along the *x*- and *z*-axes. Sliced *x*-*z* images (3 mm thick) of carbamoyl-PROXYL solution were obtained at different distances from the surface coil along the *y*-axis. The sensitivity distributions were calculated from the pixelwise enhancement of the images. **b:** OMRI signal along the *y*-axis calculated from the *y*-*z* slice OMRI image.

(200 mM in saline solution) were administered intravenously (injection time = <10 s) and the rat was inserted into the coil assembly. The OMRI scanner was immediately started. In the surface coil study, the surface coil was noninvasively positioned around the left kidney of the rat or directly fixed on the kidney after the operation on its flank. All procedures and animal care were approved by the Ethics Committee for Animal Experiments, Graduate School of Pharmaceutical Sciences, Kyushu University, and were conducted according to the guidelines for animal experiments of the Graduate School of Pharmaceutical Sciences, Kyushu University.

RESULTS AND DISCUSSION

Overhauser Enhancement of the NMR Signal Using a Surface Coil

Figure 2 shows the OMRI images (*x*-*z* plane) of the test tube containing 3 mM of carbamoyl-PROXYL solution obtained by using a surface coil for the EPR irradiation. The images obtained without the EPR irradiation (i.e., the native MR images) had a low SNR (= 5.5) due to the very low B_0 field of 14.5 mT. An EPR irradiation preceded each phase-encoding step for MRI, resulting in an increased NMR signal intensity (the SNR reached 320 at an EPR RF power of 107.8 W). The subtraction of images obtained with and without EPR irradiation yielded a difference image that showed the pure distribution of the free radical. The enhancement factors of the conventional volume coil and the surface coil at different EPR RF power levels were compared. The enhancement factor of the surface coil was calculated from values at the center of the coil on the sagittal images of the test tube. The negative sign of the enhancement factor means that the NMR signal undergoes a phase reversal upon EPR irradiation. An EPR irradiation through the surface coil resulted in a marked improvement of the irradiation efficiency compared to the conventional volume coil. The calculated EPR irradiation power needed to obtain the enhancement factor $E = -10$ is 91.3 W with a volume coil and 6.7 W with a surface coil. The unloaded

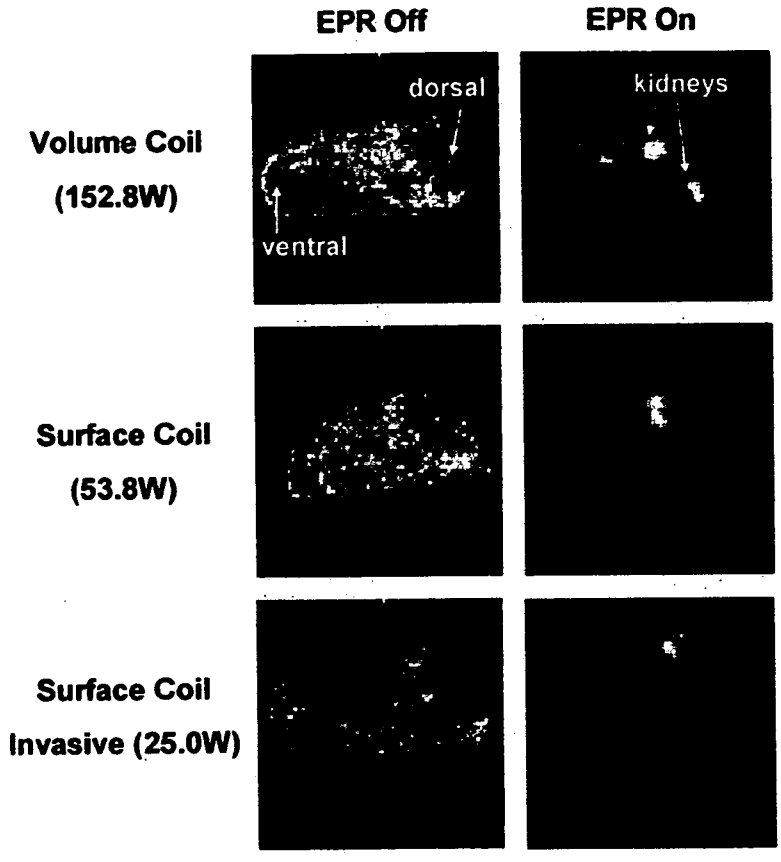

FIG. 4. OMRI images of a rat kidney detected using a volume coil or a surface coil for the EPR irradiation. Carbamoyl-PROXYL (0.8 mmol) was intravenously administered to the rat under anesthesia, and then sagittal OMRI images were obtained. In an invasive study the surface coil was directly fixed on the left kidney of the rat after the abdominal operation. Matrix size = 64 × 64, FOV = 64 × 64 mm, TR = 1200 ms, TE = 25 ms, and TEPR = 400 ms. EPR irradiation powers are shown in the figure.

quality factors of the volume and surface coils were 210 and 218, and the test-tube-loaded quality factors were 198 and 176, respectively. Equation [3] makes it possible to compare the total amount of RF power deposited into the sample during the EPR irradiation needed to obtain the same enhancement (i.e., 5.2 W with the volume coil and 1.3 W with the surface coil for $E = -10$). Accordingly, the total RF power deposition in the sample, which was averaged over the whole sample, can be reduced to 25% of volume coil by the use of the surface coil to obtain the same enhancement in this experimental condition. The difference in the total RF power deposition during the EPR irradiation for OMRI is mainly due to the difference of the saturation factor s given by Eq. [2], where B_{1e} is equal to $\Lambda P^{1/2}$. The conversion factor Λ of the volume and the surface coils when unloaded was measured using a small-loop antenna method, and the results were 5.4 and 23.9 $\mu T/W^{1/2}$, respectively, as shown in Table 1. Thus, the experimental results are consistent with the theoretical prediction that the reduction of the total RF power deposition in the sample by the surface coil is related to the ratio of the B_{1e} surface coil/B_{1e} volume coil in the localized region.

Distribution and Homogeneity of the RF Magnetic Field of the Surface Coil

The homogeneity of the B_1 field in the coil is a critical factor for MRI, and it is desirable to achieve a uniform B_1 field throughout the imaged region. We measured the B_1 homogeneity of the surface coil as an ORMI signal distribution by examining the multislice images of the test tube containing carbamoyl-PROXYL solution at various distances from the loop plane, as shown in Fig. 3a. The signal intensity decreased with the increased distance from the surface coil. This is probably due to the decrease of B_1 field strength along the y-axis direction (Fig. 3b), as expected from previous EPR imaging data (20). Though the effective distance from the loop plane on the B_1 distribution may be dependent on the RF power level used, 20% of the maximum sensitivity remains within the radius of the surface coil. The B_1 field of the surface coil showed the appropriate homogeneity for an imaging study within 5 mm from the loop plane along the x-axis. However, along the x-axis an asymmetric signal distribution was observed, and the confined region near the connection to the parallel coaxial lines had a lower B_1 field strength in the images that were more than 5 mm away from the loop plane. A conduction discontinuity in the loop current may cause such an inhomogeneity in the RF magnetic field of the surface coil.

In Vivo Performance of the Surface-Coil-Type EPR Irradiation Coil

Figure 4 shows the application of the surface-coil-type EPR irradiation coil to OMRI of a rat kidney after intravenous administration of a carbamoyl-PROXYL solution. The NMR signal is enhanced by the EPR irradiation through the conventional volume coil, and shows a bright area all over the body of the rat. Both kidneys are clearly

shown on the OMRI image, but more than 100 W of RF power was required to cause signal enhancement. EPR-on and -off images with the RF volume coil were acquired in the same rat with the same scaling, but the anatomical scaling looks different due to the so-called "negative" enhancement phenomena. The region including skin and muscle of the back has only a small concentration of free radical, which is not enough to cause positive enhancement. The signal intensity of the region with low free radical concentration is decreased compared to normal MRI (EPR-off), where it often disappears in an OMRI image. The EPR irradiation through the surface coil noninvasively attached on the side of rat also caused Overhauser enhancement of the NMR signal around the left kidney. The enhanced region was limited, but the RF power required to obtain the same enhancement in the kidney region can be reduced to about one-third of that used for the volume coil. The advantage of the surface coil on the EPR irradiation efficiency is constrained by the distance between the coil and the imaged region within 8 mm at an EPR power of 53.8 W in this experimental condition. Direct fixing of the surface coil on the kidney of rat after the surgical operation resulted in significant improvement of the EPR irradiation efficiency by a further reduction of 50% in the EPR power, considering the same enhancement value. The invasive method is useful for comparing the experimental output with the theoretical calculation, as well as for analyzing experimental disease model animals with the target organ inside the body.

The present results show that application of a surface coil to EPR irradiation is advantageous for double resonance-based Overhauser MRI, which is related to the ratio of the B_1 surface coil/B_1 volume coil in the ROI. The improved sensitivity may also be converted into a shortened EPR irradiation time, resulting in fast data acquisition. This is the reason why the surface coil has been used as a receiver coil for topical applications of MRI. The advantages of the surface coil for the rat model could be extended to human studies. However, the excessive specific absorption rate (SAR) and concomitant heating during the EPR cycle are major concerns regarding OMRI of large conducting samples. When a volume coil is used for EPR irradiation in OMRI, the "total RF power deposition into the whole body" and the "local SAR" mean almost same thing. In the case of the RF surface coil, these are different. The surface coil can reduce the total RF power deposition in the whole body and the total heating problem, but not the local SAR to obtain the same Overhauser enhancement by the volume coil. If the enhancement is the same, the local SAR in the target region should be the same no matter what kind of coil is used for EPR irradiation. Accordingly, one should carefully monitor the SAR and keep the RF power to a minimum to obtain the necessary sensitivity.

REFERENCES

1. Matsumoto K, Utsumi H. Development of separable electron spin resonance-computed tomography imaging for multiple radical species: an application to .OH and .NO. Biophys J 2000;79:3341–3349.
2. Deng Y, He G, Petryakov S, Kuppusamy P, Zweier JL. Fast EPR imaging at 300 MHz using spinning magnetic field gradients. J Magn Reson 2004;168:220–227.
3. Williams BB, Al Hallaq H, Chandramouli GV, Barth ED, Rivers JN, Lewis M, Galtsev VE, Karczmar GS, Halpern HJ. Imaging spin probe distribution in the tumor of a living mouse with 250 MHz EPR: correlation with BOLD MRI. Magn Reson Med 2002;47:634–638.
4. Placidi G, Alecci M, Sotgiu A. First imaging results obtained with a multimodal apparatus combining low-field (35.7 mT) MRI and pulsed EPRI. Phys Med Biol 2002;47:N127–N132.
5. Lurie DJ, Bussell DM, Bell LH, Mallard JR. Proton-electron double magnetic resonance imaging of free radical solutions. J Magn Reson 1988;76:366–370.
6. Krishna MC, English S, Yamada K, Yoo J, Murugesan R, Devasahayam N, Cook JA, Golman K, Ardenkjaer-Larsen JH, Subramanian S, Mitchell JB. Overhauser enhanced magnetic resonance imaging for tumor oximetry: coregistration of tumor anatomy and tissue oxygen concentration. Proc Natl Acad Sci USA 2002;99:2216–2221.
7. Li H, Deng Y, He G, Kuppusamy P, Zweier JL. Proton electron double resonance imaging of the in vivo distribution and clearance of a triaryl methyl radical in mice. Magn Reson Med 2002;48:530–534.
8. Lurie DJ, Davies GR, Foster MA, Hutchison JMS. Field-cycled PEDRI imaging of free radicals with detection at 450 mT. Magn Reson Imaging 2005;23:175–181.
9. Utsumi H, Yamada K, Ichikawa K, Sakai K, Kinoshita Y, Matsumoto S, Nagai M. Simultaneous molecular imaging of redox reactions monitored by Overhauser-enhanced MRI with 14N- and 15N-labeled nitroxyl radicals. Proc Natl Acad Sci USA 2006;103:1463–1468.
10. Ackerman JJH, Grove TH, Wong GG, Gadian DG, Radda GK. Mapping of metabolites in whole animals by 31P NMR using surface coil. Nature (Lond) 1980;283:167–170.
11. Nishikawa H, Fujii H, Berliner JL. Helices and surface coils for low-field in vivo ESR and EPR imaging applications. J Magn Reson 1985; 62:79–86.
12. He G, Samouilov A, Kuppusamy P, Zweier JL. In vivo EPR imaging of the distribution and metabolism of nitroxide radicals in human skin. J Magn Reson 2001;148:155–164.
13. Matsumoto A, Matsumoto S, Sowers AL, Koscielniak JW, Trigg NJ, Kuppusamy P, Mitchell JB, Subramanian S, Krishna MC, Matsumoto K. Absolute oxygen tension (pO(2)) in murine fatty and muscle tissue as determined by EPR. Magn Reson Med 2005;54:1530–1535.
14. Ono M, Ito K, Kawamura N, Hsieh K, Hirata H, Tsuchihashi N, Kamada H. A surface-coil-type resonator for in vivo ESR measurements. J Magn Reson Ser B 1994;104:180–182.
15. Hirata H, Walczak T, Swartz HM. Electronically tunable surface-coil-type resonator for L-band EPR spectroscopy. J Magn Reson 2000;142: 159–167.
16. Salikhov I, Hirata H, Walczak T, Swartz HM. An improved external loop resonator for in vivo L-band EPR spectroscopy. J Magn Reson 2003;164:54–59.
17. Ono M, Suenaga A, Hirata H. Experimental investigation of RF magnetic field homogeneity in a bridged loop-gap resonator. Magn Reson Med 2002;47:415–419.
18. Matsumoto S, Nagai M, Yamada K, Hyodo F, Yasukawa K, Muraoka M, Hirata H, Ono M, Utsumi H. A composite resonator assembly suitable for EPR/NMR coregistration imaging. Concepts Magn Reson B Magn Reson Eng 2005;25B:1–11.
19. Prock T, Collins DJ, Leach MO. A model to assess SAR for surface coil magnetic resonance spectroscopy measurements. Phys Med Biol 2002; 47:1805–1817.
20. He G, Evalappan SP, Hirata H, Deng Y, Petryakov S, Kuppusamy P, Zweier JL. Mapping of the B1 field distribution of a surface coil resonator using EPR imaging. Magn Reson Med 2002;48:1057–1062.

ANTIOXIDANTS & REDOX SIGNALING
Volume 9, Number 3, 2007

DOI: 10.1089/ars.2006.1502

Forum News & Views

Are Free Radical Reactions Increased in the Diabetic Eye?

MAYUMI YAMATO,[1] SHINGO MATSUMOTO,[2] KATSUAKI URA,[1]
KEN-ICHI YAMADA,[2] TATSUYA NAGANUMA,[2] TOYOSHI INOGUCHI,[3]
TOSHIAKI WATANABE,[1] and HIDEO UTSUMI[2]

ABSTRACT

Reactive oxygen species (ROS) are thought to play a significant role in the development of diabetic retinopathy; however, no direct evidence supports ROS generation *in vivo*. This study used *in vivo* electron spin resonance (ESR) spectroscopy with a surface resonator to detect local free radical reactions. The ESR signal decay of carbamoyl-PROXYL was enhanced in the eyes of streptozotocin (STZ)-induced diabetic mice. This enhanced signal decay was suppressed by the administration of SOD or the pretreatment with aminoguanidine. We demonstrate, for the first time, specific free radical reactions in the eyes of mice with STZ-induced diabetes. *Antioxid. Redox Signal.* 9, 367–373.

OXIDATIVE STRESS IN DIABETIC RETINOPATHY

CHRONIC HYPERGLYCEMIA is the major determinant of diabetic retinopathy. Cell damage caused by reactive oxygen species (ROS) is believed to play a significant role in the development of diabetic retinopathy (4). Consistent with this idea, the administration of antioxidants inhibits the development of retinopathy in diabetic rats (9, 17). The treatment of diabetic animals with aminoguanidine, aspirin, or vitamin E significantly inhibits the diabetes-induced increase in superoxide anion radical (O_2^-) production in retinal tissues and cells (4). Many reports have shown enhanced oxidative stress in diabetic retinopathy; however, it has not been proved directly in live animals.

IN VIVO ESR SPECTROSCOPY/SPIN PROBE TECHNIQUE

Nitroxyl radicals are used as spin probes in a variety of biologic experiments in which electron spin resonance (ESR) spectroscopy is used to detect ROS (13, 20–22, 28) and redox status (11). Nitroxyl radicals react with O_2^- in the presence of reducing agents (10, 19) and with hydroxy radical (•OH) (18). We proposed using nitroxyl radicals as spin probes for *in vivo* ESR spectroscopy to determine the level of ROS generation under conditions of streptozotocin (STZ)-induced diabetes mellitus (13, 20–22). In these studies, the administration of antioxidants, such as superoxide dismutase (SOD) (13, 20, 22), xanthine oxidase inhibitor (13), and NAD(P)H oxidase inhibitor (22), suppressed the enhanced signal decay. The results obtained using the *in vivo* ESR/spin-probe technique showed directly the generation of ROS in mice and rats with STZ-induced diabetes. In these studies, the animal was placed in the volume-type resonator of the ESR spectrometer to detect ROS generation in the abdomen. However, the volume-type resonator is not suitable for measuring radicals in the eyes of experimental animals, because it can detect only radicals distributed throughout a larger portion of the animal's body. Instead, a surface-coil–type resonator (surface resonator) is used to measure radicals in more restricted volumes (12, 23–25).

[1]Department REDOX Medicinal Science and [2]Department of Bio-function Science, Faculty of Pharmaceutical Sciences, and [3]Department of Medicine and Bioregulatory Science, Graduate School of Medical Science, Kyushu University, Fukuoka, Japan.

IN VIVO ESR WITH A SURFACE RESONATOR FOR DETECTION OF FREE RADICALS IN THE EYES OF LIVING MICE

To detect the free radical reactions in the eyes of living mice, we designed a surface resonator specifically for the size of the whole mouse eye. Figure 1A shows the experimental arrangement of the *in vivo* ESR spectroscopy. The mouse eye was located in the space bounded by a coil. The sensitivity was highest along the inside edge of the single-turn coil (Fig. 1B). The sensitivity decreased exponentially with increasing distance from the plane of the coil and normal to it, at any position relative to the coil.

Anesthetized mice were given 3-carbamoyl-2,2,5,5-tetramethylpyrrolindin-*N*-oxyl (carbamoyl-PROXYL) intravenously, and the ESR spectrum was measured noninvasively on the surface of the eye with the surface resonator. A typical ESR signal for carbamoyl-PROXYL of triplet lines was observed (Fig. 2A). The sensitivity map of the surface resonator indicated that the ESR signal detected with the surface resonator arose mainly from carbamoyl-PROXYL located adjacent to the whole eye. The intensity of the *in vivo* signal increased for up to 1–2 min after the injection and then gradually decreased (Fig. 2B). The decrease in the ESR signal after 2 min obeyed first-order kinetics. Conversely, when a loop-gap resonator was used for detecting the ESR signal of carbamoyl-PROXYL at head region including eyes, the maximum signal intensity was observed within 30 sec after injection (data not shown), which agreed with our previous report (15). The decay rate of the carbamoyl-PROXYL signal measured with the surface resonator was 0.07 ± 0.01 per min, and that of the probe measured with the loop-gap resonator was 0.10 ± 0.01 per min. These differences between two resonators were also confirmed by Takeshita *et al.* (25), which demonstrated that the ESR signal detected with the surface resonator was completely different

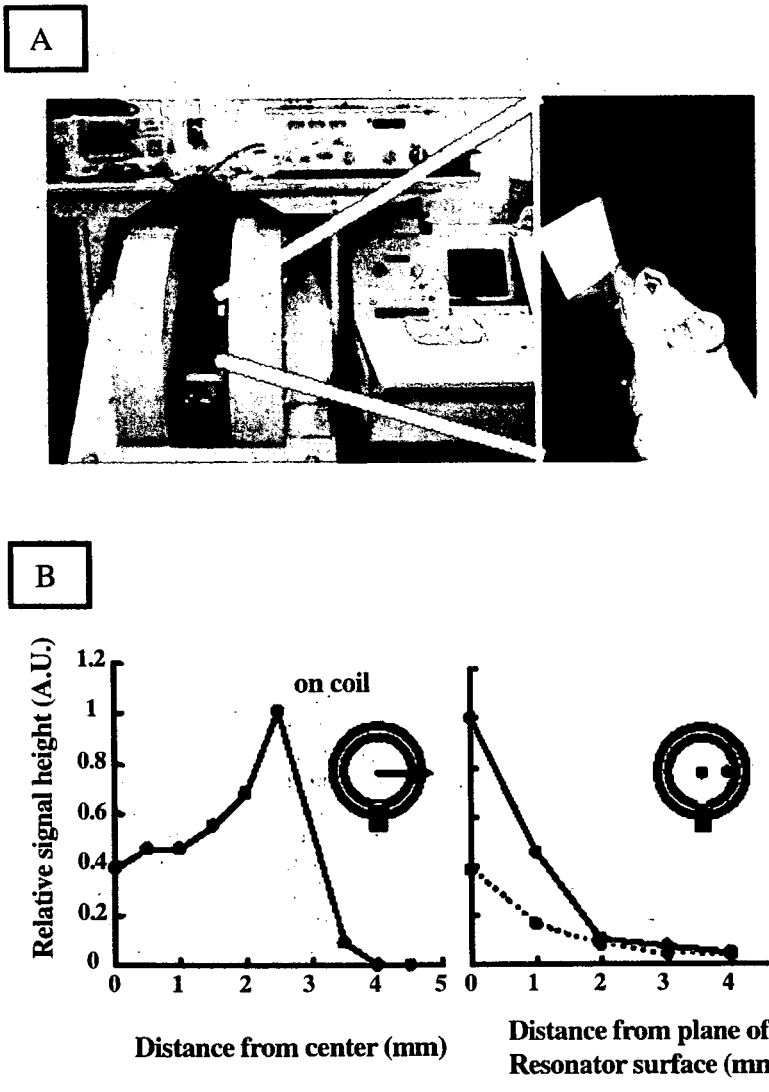

FIG. 1. L-band ESR spectrometer with a surface resonator (A) and the sensitivity distribution of the surface resonator (B). A small particle of a stable radical, 1-diphenyl-2-picrylhydrazyl radical, was placed in various positions in the plane of a single-turn loop of the surface resonator or along lines perpendicular to the resonator surface, and the relative electron spin resonance signals were measured.

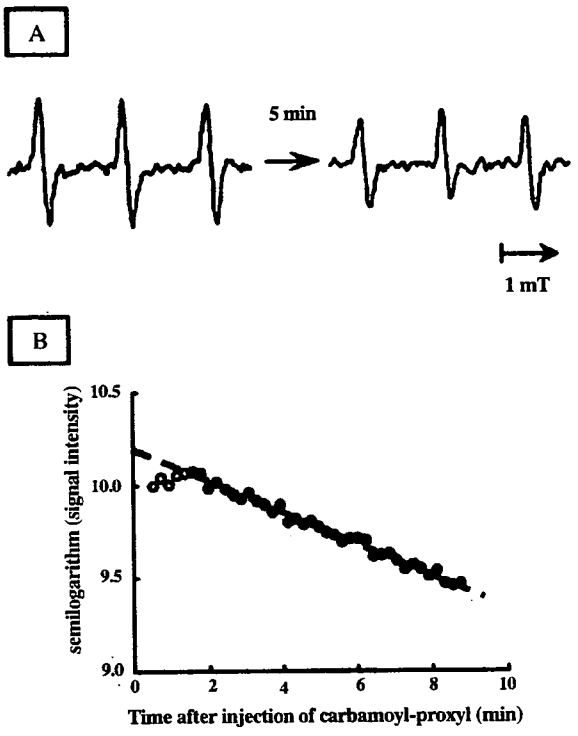

FIG. 2. Typical ESR spectrum of carbamoyl-PROXYL in the eye of a mouse (A) and the signal decay curve (B). A solution of carbamoyl-PROXYL was injected into the tail vein of the mouse.

from that of the systemic circulation and arose mainly from carbamoyl-PROXYL distributed in the skin of mouse after intravenous injection. These facts strongly suggested that surface resonator allows detection of the localized free radical.

DETECTION OF THE FREE RADICAL REACTIONS IN THE EYE OF MICE WITH STZ-INDUCED DIABETES

The body weight, glucose concentration, creatinine concentration, and fructosamine concentration in the plasma of STZ- and vehicle-treated mice are shown in Table 1. The blood glucose in the diabetic mice was approximately twice that in the vehicle-treated group after STZ treatment. The yield of colored formazan dye, which was calibrated using a fructosamine standard curve, was significantly higher than that in vehicle-treated mice 4 weeks after STZ treatment.

To provide direct evidence that the eyes of STZ-treated mice produce more ROS *in vivo* than the eyes of control mice, the *in vivo* ESR/spin-probe technique was applied to STZ- and vehicle-treated mice. A semilogarithmic plot of the signal intensity versus time was almost linear from 2 to 7 min after injection, allowing calculation of the initial velocity as the signal-decay rate (Fig. 3). The signal decay was clearly faster in the STZ-treated mouse than in the vehicle-treated mouse at 4 weeks after STZ treatment (Fig. 3A). The signal decay of the upper abdomen was enhanced at 2 weeks after STZ treatment in previous reports (13, 20, 22), but no detectable change in the eye was found at this earlier time point.

The previous results indicated that ROS generation, monitored with the *in vivo* ESR/spin-probe technique, was enhanced in STZ-treated mice and rats and that the enhanced ROS generation was related to hyperglycemia (13, 20, 22). In the present experiments, the simultaneous injection of SOD with carbamoyl-PROXYL completely suppressed the enhanced signal decay in the STZ-treated mice (Fig. 3B). These results suggest that enhanced free radical reactions were responsible for the enhanced signal decay observed in the eyes of STZ-treated mice. Peroxynitrite may also contribute to the enhanced signal decay, because SOD also inhibits peroxynitrite generation caused by the disproportion of O_2^-.

NONENZYMATIC GLYCATION REACTION AS SOURCE OF ROS

Nonenzymatic glycation is a reaction between glucose and an amino group in a protein that results in the creation of a ketoamine, and it leads to the formation of Amadori products such as fructosamine. Amadori products and derived reactive carbonyl compounds are known to generate oxygen free radicals (16). Although the glycation reaction is reversible *in vitro* and *in vivo* under normoglycemia resulting from improved glycemic control, oxygen free radicals accelerate the formation of irreversible and highly reactive adducts, the so-called advanced glycosylation end products (AGEs), and

TABLE 1. GENERAL CHARACTERISTICS OF MICE WITH STZ-INDUCED DIABETES

	2 week		*4 week*	
	Control	*Diabetic mice*	*Control*	*Diabetic mice*
Body weight (g)	38.6 ± 0.5	37.2 ± 0.7	43.8 ± 1.2	33.9 ± 1.7[b]
Glucose (mg/dl)	182.7 ± 7.8	425.3 ± 59.4[a]	196.9 ± 9.9	442.8 ± 31.1[b]
Fructosamine (μ*M*)	499.4 ± 34.0	617.2 ± 42.6	505.6 ± 18.7	666.8 ± 55.7[c]
Creatinine (mg/dl)	0.82 ± 0.09	0.87 ± 0.09	0.88 ± 0.05	0.84 ± 0.05

Each value represents the mean ± SEM.
[a] $p < 0.005$ *vs.* the 2-weenondiabetic group.
[b] $p < 0.005$ and [c] $p < 0.05$ *vs.* the nondiabetic group at 4 weeks after the injection. Eight animals were used for each experiment.

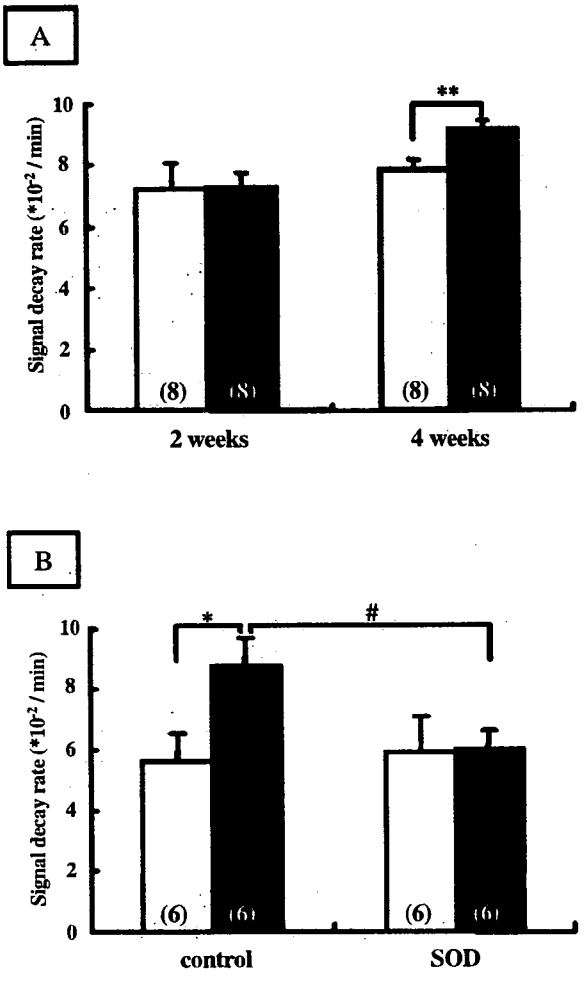

FIG. 3. Changes in the signal-decay rate in mice with STZ-induced diabetes compared with nondiabetic control mice (A) and the effect of SOD on the signal-decay rate 4 weeks after STZ treatment (B). Two and 4 weeks after the onset of diabetes, *in vivo* ESR measurements were performed. The carbamoyl-PROXYL signal-decay curve was obtained by plotting the peak height of the ESR signals semilogarithmically. The initial kinetic constant (signal-decay rate) was calculated from the slope of the signal-decay curve. *Open columns* indicate vehicle-treated mice, and *solid columns* indicate STZ-treated mice. The values in parenthesis are the numbers of animals. Each value represents the mean ± SEM; $*p < 0.05$ and $**p < 0.01$ *vs.* the nondiabetic group; and $^{\#}p < 0.05$ vs. the diabetic group treated with saline instead of SOD.

cause cross-links in protein. AGE formation is hypothesized to function in the development of diabetic cataract, and therefore pharmacologic agents have been sought to inhibit this process by blocking the glycation cascade. The nucleophilic hydrazine compound aminoguanidine is the most extensively investigated compound of this type and effectively inhibits AGE formation. Thus, combining the *in vivo* ESR/spin-probe technique with aminoguanidine should reveal the relation between glycation and the formation of *in vivo* free radical reactions in the STZ-induced diabetic cataract.

To confirm the contribution of the nonenzymatic glycation cascade to the increased free radical reaction, the mice were treated with aminoguanidine. The aminoguanidine distinctly suppressed the enhanced signal decay (Fig. 4A) in the STZ-treated mice. Plasma collected 4 weeks after STZ treatment yielded colored formazan dye from NBT (Fig. 4B). Formazan dye is generated by reactive species such as O_2^- (8) and Amadori products (7). Aminoguanidine reacts with reactive carbonyl groups, resulting in decreased NBT reduction (1). Some correlation was observed between the enhanced signal decay

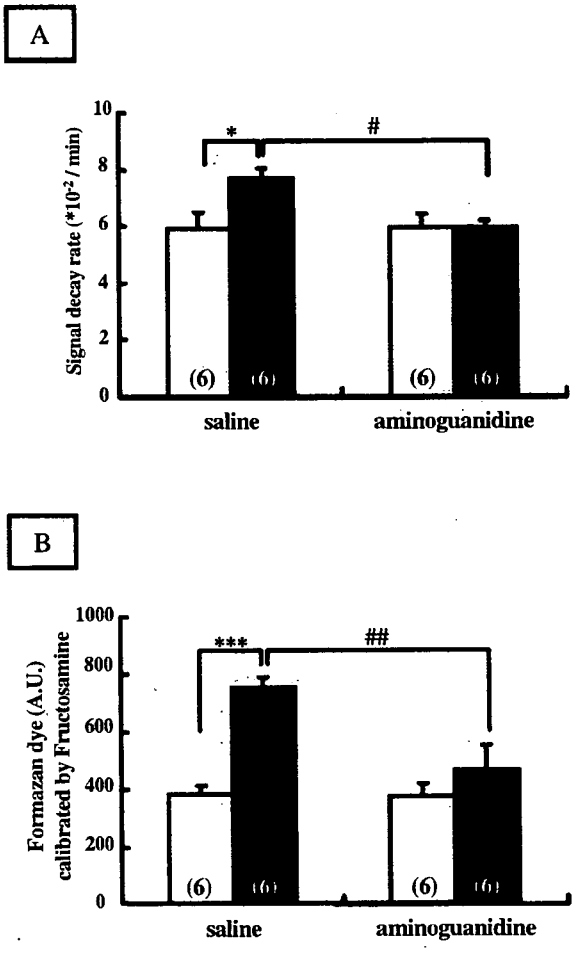

FIG. 4. Effect of aminoguanidine on the *in vivo* free radical reaction (A) and the yield of colored formazan dye (B). Aminoguanidine (100 mg/kg body weight) was intraperitoneally injected once daily on each Monday through Friday from 2 to 4 weeks after the onset of diabetes. *Open columns* indicate vehicle-treated mice, and *solid columns*. STZ-treated mice. The values in parenthesis are the numbers of animals. Each value represents the mean ± SEM; $*p < 0.05$ and $***p < 0.005$ *vs.* the nondiabetic group; and $^{\#}p < 0.05$ and $^{\#\#}p < 0.01$ *vs.* the diabetic group treated with saline instead of aminoguanidine.

and the yield of colored formazan dye ($R = 0.606$; $p < 0.026$; $n = 12$). These findings suggest that aminoguanidine inhibits free radical reactions via the nonenzymatic glycation cascade.

CONCLUSIONS AND OPEN QUESTIONS

This study detected free radical reactions in the whole eyes of living mice and confirmed that free radical reactions occur in the eyes of STZ-treated mice. To perform the experiments, we designed a surface resonator specifically for the size of the whole mouse eye. The mouse eye was located in the space bounded by a coil. We previously confirmed that the signal decay rates of carbamoyl-PROXYL varied at different regions, and the enhancement of signal decay limited to the region exposed to oxidative stress, although details are unclear (25–28). For example, in adjuvant arthritis model rats, any difference was not observed in the signal-decay rate between arthritis model and control group at the breast and abdomen, although significant enhancement was observed at the paw (27). When we used carbamoyl-PROXYL as a spin probe, the probe allowed us to detect ROS generation not in systemic circulation but at the interface of the cell membrane (28). We also confirmed that the surface resonator was sensitive only to the plane of the coil, and the sensitivity of the surface resonator was limited to the signal of carbamoyl-PROXYL distributed to the eye.

The ESR signal decay of carbamoyl-PROXYL in the eye was enhanced in mice with STZ-induced diabetes. We previously proposed using nitroxyl radicals as spin probes for *in vivo* ESR spectroscopy to determine the level of ROS generation under conditions of STZ-induced diabetes mellitus (13, 20). In these studies, the signal decay at the upper abdomen was enhanced at 2 weeks after STZ treatment, and the enhanced signal decay was related to hyperglycemia. However, in the present study, no detectable change of signal decay was found in the eye at this earlier time point, although the concentration of blood glucose in the diabetic group was higher than that of control. Interestingly, the signal decay in the eye enhanced at 4 weeks after STZ treatment when the formazan dye calibrated by fructosamine was increased. These results suggested that mechanisms of oxidative stress in the eye may be different from those of in the upper abdomen.

The enhanced signal decay was suppressed by the administration of SOD, indicating that increased free radical reactions largely accounted for the enhanced signal decay. This observation was similar to previous results demonstrating enhanced signal decay in the abdomen (13, 20–22). The reaction of carbamoyl-PROXYL with O_2^- likely occurs mainly within the lumen of capillaries in the eye, because membrane-impermeable reagents such as SOD completely inhibited the enhanced signal decay of the probe. Various mechanisms have been postulated for intravascular O_2^- generation (13, 22).

The glycation of biologic substances seems to contribute to ROS generation. Mullarkey *et al.* (16) confirmed that O_2^- was generated by the glycation of proteins, using the ESR/spin-trap technique. A diabetes-like glucose concentration increases the O_2^- production in retinal cells, and the O_2^- contributes to impaired viability and increased cell death under these circumstances (4).

The colored formazan dye is generated by the reduction of NBT by ketoamines in alkaline solution (1, 2, 7). The nucleophilic aminoguanidine can react with a reactive carbonyl groups (6), lowering the amount of NBT reduction. Aminoguanidine does not change the concentration of hemoglobin A1c, which is determined by a relatively direct method such as high-performance liquid chromatography (HPLC) or immunochemistry (3). The carbonyl structures of Amadori products may contribute to the *in vivo* free radical reactions that we confirmed using the *in vivo* ESR/spin-probe technique (Fig. 4). Hence, the reaction between aminoguanidine and the reactive carbonyls of glycation adducts may be one of the mechanisms for the inhibitory action of aminoguanidine on the free radical reactions and subsequent AGE formation. Conversely, aminoguanidine also inhibits inducible nitric oxide synthase (14) and scavenges peroxynitrite (29), so the generation of RNS in the eye might contribute to the *in vivo* free radical reactions.

We used a surface-type ESR resonator for the *in vivo* detection of free radical reactions in the whole eye. This is the first report of the *in vivo* detection of free radical reactions occurring in the eye of a living animal. *In vivo* ESR spectroscopy is likely to be useful in retinopathy, not only for studying the mechanism of injury through free radical reactions but also for screening drugs such as aminoguanidine.

ABBREVIATIONS

AGE, advanced glycosylation end product; carbamoyl-PROXYL, 3-carbamoyl-2,2,5,5-tetramethylpyrrolindin-*N*-oxyl; ESR, electron spin resonance; NBT, nitroblue tetrazolium; ROS, reactive oxygen species; SOD, superoxide dismutase; STZ, streptozotocin; surface resonator, surface-coil-type resonator.

APPENDIX

Notes

1. Chemicals

Streptozotocin (STZ), the creatinine assay kit, the glucose assay kit, and uricase were purchased from Wako Pure Chemical Industries (Osaka, Japan). Aminoguanidine, nitroblue tetrazolium (NBT), and SOD were purchased from Sigma-Aldrich Co. (St. Louis, MO), and 3-carbamoyl-2,2,5,5-tetramethylpyrrolidine-*N*-oxyl (carbamoyl-PROXYL) was from Aldrich Chemical Co. (Milwaukee, WI). The fructosamine standard was purchased from Roche Diagnostics Japan. All other chemicals were of the highest grade.

2. Animals

Female ICR mice (age 4 weeks) were obtained from Kyudo Co., Ltd. (Fukuoka, Japan) and were acclimated for 1 week before the experiments. Diet (MF; Oriental Yeast Co. Tokyo, Japan) and water were provided *ad libitum*. At 5 weeks of age, 80 mg/kg body weight of STZ in saline was injected into the tail vein of the mice after overnight fasting, as described previously (13). Vehicle-treated animals received only saline. The mice were used for the following experiments 2 or 4 weeks after the onset of diabetes. All procedures and animal care were approved by the Committee on Ethics of Animal Experiments, Graduate School of Pharmaceutical Sciences, Kyushu University, and were conducted according to the Guidelines for Ani-

mal Experiments of the Graduate School of Pharmaceutical Sciences, Kyushu University.

3. *In vivo* ESR measurement

An electrically tunable surface resonator consisting of a single-turn coil (6 mm in diameter), a parallel semirigid coaxial line, and matching and tuning circuits (5) was connected to an L-band ESR spectrometer (JES RE-3L; JEOL, Akishima, Japan), and a handmade 100-kHz field modulation coil was attached to the surface of the ESR magnet.

Mice were anesthetized with intraperitoneal injection of pentobarbital and placed in a handmade holder. An isotonic solution containing 150 m*M* carbamoyl-PROXYL (2.4 mmol/kg body weight) as the spin probe was injected into the tail vein, and a surface resonator was then gently attached to the eye to be examined, and ESR spectra were recorded at 12-s intervals for 10 min.

SOD (10 units/mouse) was administered simultaneously with the carbamoyl-PROXYL. Aminoguanidine (100 mg/kg body weight) was intraperitoneally injected once daily, Monday through Friday, from 2 to 4 weeks after the onset of diabetes.

4. Plasma glucose, uric acid, creatinine, and formazan dye assays

Blood was collected, heparinized, and then spun for 10 min at 900 *g*. The plasma glucose, uric acid, and creatinine concentrations were determined using an assay kit for each. The change from NBT to formazan was used as an assay to evaluate Amadori products such as fructosamine (7). Plasma was added to carbonate buffer at pH 10.3 containing NBT (0.54 m*M*) in the presence of uricase (3.78 units/ml). The absorbance at 546 nm was measured 10 and 15 min after mixing and compared with a fructosamine standard (412 μ*M*). The whole assay was carried out at 37°C.

5. Statistical analysis

Each value represents the mean ± SEM. Significant differences were determined by one-way analysis of variance (ANOVA) using the Tukey *post hoc* test. Pearson's coefficient test was used to determine correlations. Values of $p < 0.05$ were accepted as statistically significant.

ACKNOWLEDGMENTS

This work was supported by Grants-in-Aid for Scientific Research from the Ministry of Education, Science, Sports, and Culture of Japan and the Mitsubishi Pharma Corporation. We thank Dr. Hiroshi Hirata of Yamagata University for technical advice on the surface-coil–type resonator.

REFERENCES

1. Baker JR, Zyzak DV, Thorpe SR, and Baynes JW. Chemistry of the fructosamine assay: D-glucosone is the product of oxidation of Amadori compounds. *Clin Chem* 40: 1950–1955, 1994.
2. Baker JR, Zyzak DV, Thorpe SR, and Baynes JW. Mechanism of fructosamine assay: evidence against role of superoxide as intermediate in nitroblue tetrazolium reduction. *Clin Chem* 39: 2460–2465, 1993.
3. Bolton WK, Cattran DC, Williams ME, Adler SG, Appel GB, Cartwright K, Foiles PG, Freedman BI, Raskin P, Ratner RE, Spinowitz S, Whittier FC, and Wuerth JP. Randomized trial of an inhibitor of formation of advanced glycation end products in diabetic nephropathy. *Am J Nephrol* 24: 32–40, 2004.
4. Du Y, Miller CM, and Kern TS. Hyperglycemia increases mitochondrial superoxide in retina and retinal cells. *Free Radic Biol Med* 35: 1491–1499, 2003.
5. Hirata H, Walczak T, and Swartz HM. Electronically tunable surface-coil-type resonator for L-band EPR spectroscopy. *J Magn Reson* 142: 159–167, 2000.
6. Hirsch J, Petrakova E, and Feather MS. The reaction of some dicarbonyl sugars with aminoguanidine. *Carbohydr Res* 232: 125–130, 1992.
7. Johnson RN, Metcalf PA, and Baker JR. Fructosamine: a new approach to the estimation of serum glycosylprotein: an index of diabetic control. *Clin Chim Acta* 127: 87–95, 1983.
8. Johnston RB Jr, Keele BB Jr, Misra HP, Lehmeyer JE, Webb LS, Baehner RL, and RaJagopalan KV. The role of superoxide anion generation in phagocytic bactericidal activity. studies with normal and chronic granulomatous disease leukocytes. *J Clin Invest* 55: 1357–1372, 1975.
9. Kowluru RA, Koppolu P, Chakrabarti S, and Chen S. Diabetes-induced activation of nuclear transcriptional factor in the retina, and its inhibition by antioxidants. *Free Radic Res* 37: 1169–1180, 2003.
10. Krishna MC, Grahame DA, Samuni A, Mitchell J B, and Russo A. Oxoammonium cation intermediate in the nitroxide-catalyzed dismutation of superoxide. *Proc Natl Acad Sci U S A* 89: 5537–5541, 1992.
11. Kuppusamy P, Li H, Ilangovan G, Cardounel AJ, Zweier JL, Yamada K, Krishna MC, and Mitchell JB. Noninvasive imaging of tumor redox status and its modification by tissue glutathione levels. *Cancer Res* 62: 307–312, 2002.
12. Kuppusamy P, Wang P, Shankar RA, Ma L, Trimble CE, Hsia CJ, and Zweier JL. In vivo topical EPR spectroscopy and imaging of nitroxide free radicals and polynitroxyl-albumin. *Magn Reson Med* 40: 806–811, 1998.
13. Matsumoto S, Koshiishi I, Inoguchi T, Nawata H, and Utsumi H. Confirmation of superoxide generation via xanthine oxidase in streptozotocin-induced diabetic mice. *Free Radic Res* 37: 767–772, 2003.
14. Misko TP, Moore WM, Kasten TP, Nickols GA, Corbett JA, Tilton RG, McDaniel ML, Williamson JR, and Currie MG. Selective inhibition of the inducible nitric oxide synthase by aminoguanidine. *Eur J Pharmacol* 233: 119–125, 1993.
15. Miura Y, Utsumi H, and Hamada A. Effects of inspired oxygen concentration on in vivo redox reaction of nitroxide radicals in whole mice. *Biochem Biophys Res Commun* 182: 1108–1114, 1992.
16. Mullarkey CJ, Edelstein D, and Brownlee M. Free radical generation by early glycation products: a mechanism for accelerated atherogenesis in diabetes. *Biochem Biophys Res Commun* 173: 932–939, 1990.
17. Rota R, Chiavaroli C, Garay RP, and Hannaert P. Reduction of retinal albumin leakage by the antioxidant calcium dobesilate in streptozotocin-diabetic rats. *Eur J Pharmacol* 495: 217–224, 2004.
18. Samuni A, Goldstein S, Russo A, Mitchell JB, Krishna MC, and Neta P. Kinetics and mechanism of hydroxyl radical and OH-adduct radical reactions with nitroxides and with their hydroxylamines. *J Am Chem Soc* 124: 8719–8724, 2002.
19. Samuni A, Krishna CM, Mitchell JB, Collins CR, and Russo A. Superoxide reaction with nitroxides. *Free Radic Res Commun* 9: 241–249, 1990.
20. Sano T, Umeda F, Hashimoto T, Nawata H, and Utsumi H. Oxidative stress measurement by in vivo electron spin resonance spectroscopy in rats with streptozotocin-induced diabetes. *Diabetologia* 41: 1355–1360, 1998.
21. Sonta T, Inoguchi T, Matsumoto S, Yasukawa K, Inuo M, Tsubouchi H, Sonoda N, Kobayashi K, Utsumi H, and Nawata H. In vivo imaging of oxidative stress in the kidney of diabetic mice and its normalization by angiotensin II type 1 receptor blocker. *Biochem Biophys Res Commun* 330: 415–422, 2005.
22. Sonta T, Inoguchi T, Tsubouchi H, Sekiguchi N, Kobayashi K, Matsumoto S, Utsumi H, and Nawata H. Evidence for contribution of vascular NAD(P)H oxidase to increased oxidative stress in animal models of diabetes and obesity. *Free Radic Biol Med* 37: 115–123, 2004.
23. Swartz HM, Liu K J, Goda F, and Walczak T. India ink: a potential clinically applicable EPR oximetry probe. *Magn Reson Med* 31: 229–232, 1994.
24. Takeshita K, Chi C, Hirata H, Ono M, and Ozawa T. In vivo generation of free radicals in the skin of live mice under ultraviolet light, measured by L-band EPR spectroscopy. *Free Radic Biol Med* 40: 876–885, 2006.

25. Takeshita K, Takajo T, Hirata H, Ono M, and Utsumi H. In vivo oxygen radical generation in the skin of the protoporphyria model mouse with visible light exposure: an L-band ESR study. *J Invest Dermatol* 122: 1463–1470, 2004.
26. Utsumi H, Yasukawa K, Soeda T, Yamada K, Shigemi R, Yao T, and Tsuneyoshi M. Noninvasive mapping of reactive oxygen species by in vivo electron spin resonance spectroscopy in indomethacin-induced gastric ulcers in rats. *J Pharmacol Exp Ther* 317: 228–235, 2006.
27. Yamada K, Nakamura T, and Utsumi H. Enhanced intraarticular free radical reactions in adjuvant arthritis rats. *Free Radic Res* 40: 455–460, 2006.
28. Yamato M, Egashira K, and Utsumi H. Application of in vivo ESR spectroscopy to measurement of cerebrovascular ROS generation in stroke. *Free Radic Biol Med* 35: 1619–1631, 2003.
29. Yildiz G, Demiryurek AT, Sahin-Erdemli I, and Kanzik I. Comparison of antioxidant activities of aminoguanidine, methylguanidine and guanidine by luminol-enhanced chemiluminescence. *Br J Pharmacol* 124: 905–910, 1998.

Address reprint requests to
Hideo Utsumi
Department of Bio-function Science
Faculty of Pharmaceutical Sciences
Kyushu University
Fukuoka 812–8582, Japan

E-mail: utsumi@pch.phar.kyushu-u.ac.jp

Date of first submission to ARS Central, November 9, 2006; date of acceptance, November 10, 2006.

第30回日本高血圧学会総会

永大循内
乙岡

高血圧学の進歩をすべての人に
―心血管病攻略の新しいステージへ―

プログラム・抄録集

平成19年10月25日（木）～27日（土）
沖縄コンベンションセンター

The 30th Annual Scientific Meeting of
the Japanese Society of Hypertension

Program and Abstracts

Okinawa Convention Center
Oct. 25-27, 2007 Okinawa Japan

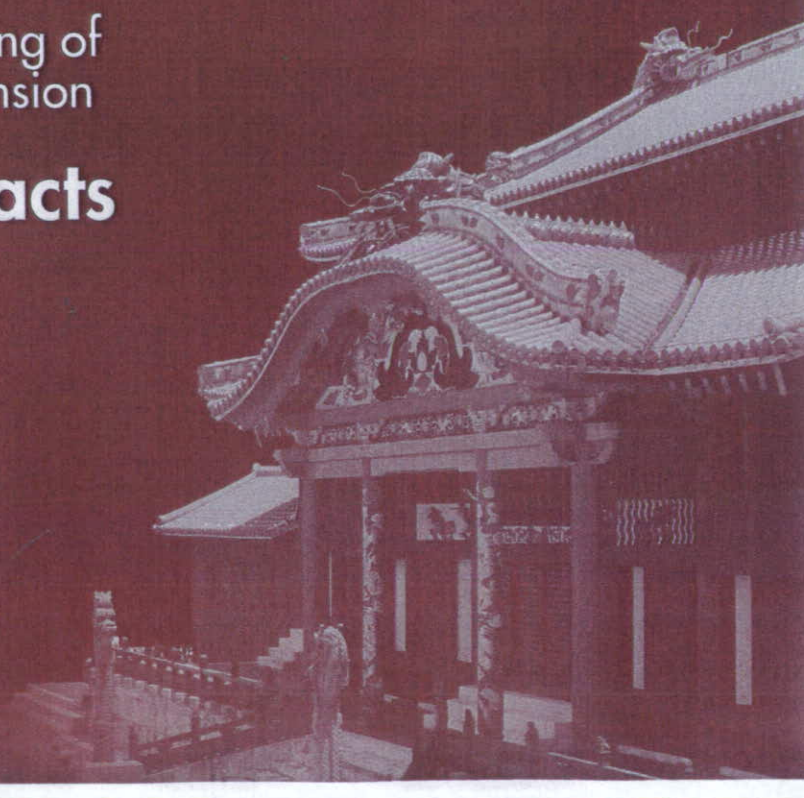

日本高血圧学会

E-10 血圧調節機構の根幹に迫る：中枢・交感神経の研究

廣岡　良隆
九州大学大学院医学研究院 循環器内科学

血圧調節において交感神経系はレニン・アンジオテンシン系と並んで重要な二大制御系のひとつである。交感神経系の活性化やストレスなど刺激に対する過剰な反応が高血圧の病態で問題であり、動脈硬化の進展や心肥大から臓器障害が生じる。

交感神経調節機構を理解するためには、如何にして交感神経活動が制御されているか、高血圧ではどのような異常が生じているがため高い血圧が容認されているのか、を知らなければならない。瞬時の血圧は動脈圧受容器反射によって一定の値に戻そうと制御されている。実際に、血圧と交感神経活動を記録して刺激を加えた際のこれらの応答をみると極めて巧妙にできているものだと学生の時に教科書で読んだだけのたった一行くらいの記述に感動する。つい最近までそれらの応答を調べた研究が多かったわけだが、高血圧や心不全における交感神経活動亢進の仕組みはわからなかった。そこで、登場したのが心血管中枢と呼ばれる頭側延髄腹外側野(RVLM)である。ここを局所的に刺激すると劇的な昇圧反応が生じ、また、破壊すると血圧は脊髄レベルとなり生命が絶たれる。この部位の発見は以後の研究を大きく発展させた。特に、交感神経系に対してこれまで、脳にまでさかのぼった形での研究は難しかったが、最近はそのようなアプローチがなされるようになり、いろいろなことがわかってきた。その結果、血圧の異常は、末梢血管抵抗などの血管の反応によるだけではなく、そもそも脳内にそれを規定する場所としてRVLMがあり、そこに常が存在すると考えられるようになった。

そこでわれわれは正常血圧ラット及び高血圧モデルラットを用いて脳内の活動を変化させることを試みた。無麻酔覚醒下で脳内局所に関連する遺伝子を導入し、脳内の特定の遺伝子の発現及びその産生物質を変化させたところ、全身の血圧を数日以上にわたって変化させることができた。そして、脳内の一酸化窒素、活性酸素、Rho-kinaseなどの役割を明らかにしてきた。

本セッションでは、この分野の研究がどのように進んできたか、われわれの研究室で論文発表された研究内容に触れながらその主役を果たしてきた大学院生・研究生がどのような努力・工夫をしたか、喜びを得たか、世界での動向・今後の展開などを紹介する。

E-11 プロとしてのモチベーション

深水　昭吉
筑波大学 先端学際領域研究センター

何のために？

皆さんは、何のために医師になりましたか？　そして、何のために高血圧学会に参加していますか？

医学部に入学した時から、多くの学生さん達が医師を目指すことになります。すなわち、医に携わる者としての知識を授かり、他学部を卒業した人達と大きく違い、卒業時から医師としてプロ意識を持つはずです。

プロフェッショナルとは？

野茂英雄によってアメリカ大リーグへの道が大きく拓かれて以来、イチロー、松井秀喜や松坂大輔をはじめとした選手達が大活躍していることはご存知の通りです。彼らは、自分の持てる力(場合によっては才能)を維持・向上させるために節制し、トレーニングを欠かしません。時には、打撃・投球フォームの改造に取り組み、探求心を持って、日々ベースボールを“研究”しています。そして、病気の子供達を励まし、人々に勇気と夢と希望を与え、常に社会に対して何が出来るかを考えています。これこそが、メジャーリーガーのプロ意識です。

モチベーション

しかし、何十億円の年俸をもらっている人達だけがプロなのではなく、医療従事者も研究者も立派なプロです。私は、ゲノム機能に大変興味を持ち、その謎を解明しようと基礎研究を推進しています。自分の興味を満たすだけのためではなく、必ず多くの方々に役立つことを信じて取り組んでいますが、研究を始めた当初は、高血圧トランスジェニック動物作製・解析の競争に大きく遅れ、挫折と自信喪失の繰り返しでした。そのような中でも、恩師の先生や共同研究者の方々のお陰で、研究をやり遂げたという“達成感”と貴重な“成功体験”を味わうことができ、研究推進のモチベーションになりました。この点を、教育セッションでお話ししたいと思います。

また、生命の進化と連動してきたゲノム情報を解明することは、果てしなく長い年月がかかります。到底一代では成し遂げることが出来ませんので、次世代の若い研究者の育成の一翼を担うことも、プロとしてのモチベーションになっています。

さて、ローマの哲人皇帝マルクス・アウレリウスは、「自分自身が何をなすべきかを知らない人間が、どうして他人に、何をなすべきかを教えることができよう!」と述べています。この言葉を借りるならば、常に問題意識を持ち、あらゆる手段を考案し、その問題解決に向けて取り組むことがプロだと考えます。そこで、最初の質問を違うアングルから伺いますが、皆さんはプロの医師として、高血圧学会に参加するモチベーションは何ですか？

BO-33 自然発症高血圧ラットへの食塩負荷による血圧上昇には頭側延髄腹外側野におけるレニンアンギオテンシン系、NAD(P)H oxidase活性の亢進を伴う活性酸素種増加が関与する

古閑 靖章、廣岡 良隆、荒木 周一郎、野副 純世、相良 洋治、岸 拓弥、砂川 賢二
九州大学大学院医学研究院 循環器内科学

【目的】自然発症高血圧ラット(SHR)に高濃度の食塩負荷を行うと、交感神経活動亢進・血圧上昇が増強するが、その機序は未だ不明な点が多い。我々は脳卒中易発症性自然発症高血圧ラットにおいて、交感神経活動の中枢である頭側延髄腹外側野(RVLM)で活性酸素種(ROS)が増加しており、RVLMでのROSの増加が高血圧の中枢性機序において極めて重要であると報告した。また、中枢でのROSの増加が、脳内レニン・アンジオテンシン(RAA)系やNAD(P)H oxidaseの活性化によるものであるという報告が相次いでいる。そこで本研究では、高濃度食塩負荷(8%食塩:HS)を行ったSHRのRVLMにおいて、食塩負荷による血圧上昇に中枢のROSが関与しているか、その機序に同部位におけるRAA系、NAD(P)H oxidase活性の亢進が関与しているかの検討を行った。【方法】雄性6週齢のSHRをHSと通常食塩負荷(0.5%食塩:RS)の2群に分け、コントロール群としてRSを与えた正常血圧ラット(WKY)を、6週間血圧を観察した。ROSの指標として過酸化脂質(TBARS)を、交感神経活動の指標として24時間蓄尿による尿中ノルエピネフリン(NE)量測定を行った。RVLMにおけるアンジオテンシンII type1受容体蛋白の発現をウェスタンブロット法で測定し、NAD(P)H oxidase活性の測定も行った。【成績】収縮期血圧は8週齢目よりHS-SHRでRS-SHRと比べ有意な上昇を認めた(214±4mmHg vs 172±4mmHg, n=8, P<0.05)。12週齢時のRVLMにおけるTBARSは、SHR両群でWKYと比べ高値であり、HS-SHRではRS-SHRと比べ有意な増加を認めた(9.9±0.5μmol/g wet wt vs 8.1±0.6μmol/g wet wt, n=5, P<0.05)。両側RVLMへの活性酸素消去酵素であるTempol微量投与実験ではHS-SHRでRS-SHRと比べ有意に大きな血圧降下応答を認めた。尿中NE量は、HS-SHRでRS-SHRと比べ有意な増加を認めた(2.09±0.10μg vs 1.47±0.05μg, n=5, P<0.05)。Hexamethoniumの静脈内投与では、HS-SHRでRS-SHRに比べ有意に大きな降圧反応を認め、同レベルまで血圧低下を認めた。RVLMにおけるアンジオテンシンII type1受容体蛋白の発現はHS-SHRでRS-SHRに比べ有意に増加しており、NAD(P)H oxidase活性も亢進している傾向を認めた。【結論】以上の成績は、SHRへの高濃度食塩負荷はRVLMでのROSの増加により、さらに交感神経活動亢進・血圧上昇を認め、これには中枢でのRAA系の活性化、NAD(P)H oxidase活性の亢進が関与していることを示唆する。

BO-34 新規の昇圧物質coupling factor 6の細胞内情報伝達機構とカルシウムシグナル

長内 智宏、芦立 俊宗、斎藤 新、山田 雅大
弘前大学 循環呼吸腎臓内科学

【目的】Coupling factor 6(CF6)はミトコンドリアATP合成酵素の1つのcomponentであり、ATP産生に促進的に作用する。最近、我々はCF6が血管内皮細胞のprostacyclin産生を抑制し、昇圧活性を有することを報告した。更に、本態性高血圧患者において血中CF6濃度が高値を示し、食塩感受性と関連を有することを明らかにした。CF6の血管内皮細胞における細胞内情報伝達機構は解明されたが、血圧に直接関与する血管平滑筋細胞(VSMC)の情報伝達機構は不明である。本研究の目的は、CF6のVSMCにおける細胞内情報伝達機構、Ca signal、ならびに高血圧への関与を明らかにすることである。【方法】1) VSMC:高血圧自然発症ラット(SHR)と正常血圧ラット(WKY)の腸間膜動脈VSMCならびに電位依存性Caチャネルの恒常的発現細胞A7r5(ラット大動脈VSMC)を使用した。2) CF6結合アッセイ:^{125}I-CF6を添加し、37℃で30分保温後、結合型^{125}I-CF6をcountした。ATP、ADP、ATP合成酵素α-subunit並びにβ-subunit抗体の^{125}I-CF6結合に及ぼす影響について検討した。3) ATPase活性:ATPを添加しADPへの分解速度を、NADHの酸化反応系を用いて測定した。4) 細胞内pHの測定:BCECFをloadし、励起波長495 nm並びに440 nm、蛍光波長535 nmで測定した。5) c-Src活性化:c-Src tyrosineリン酸化をWestern blot法で測定した。6) 細胞内遊離Ca濃度の測定:Fura-2をloadし、励起波長340 nm並びに380 nm、蛍光波長500 nmで測定した。【成績】1) Competitive displacement analysisより求めたCF6受容体のKd値はSHRがWKYに比較して小であった(3.6±0.3 vs 9.6±0.3 nM, p<0.05)。^{125}I-CF6結合はβ-subunit抗体とADPにより有意に抑制された。2) ATPase活性は、CF6 10^{-7}M投与により上昇し、SHRがWKYに比較して大であった(58.1±7.6 vs 34.6±8.4%, p<0.05)。3) 細胞内pHはCF6 10^{-7}M投与により低下し、その低下はSHRがWKYに比較して大であった(0.26±0.03 vs 0.13±0.02, p<0.05)。CF6による細胞内pHの低下は、ATPase阻害薬efrapeptin 10^{-5}Mの前投与により完全に抑制された。4) c-SrcはCF6 10^{-7}M投与によりtyrosine残基がリン酸化され、その反応はSHRがWKYに比較して2倍大であった。5) A7r5細胞にCF6 10^{-7}Mを添加すると、細胞内遊離Ca濃度の上昇が認められ、nifedipine投与により完全に抑制された。Angiotensin II(AngII)10^{-7}Mによる細胞内遊離Ca濃度の上昇はCF6 10^{-7}M前投与により増強され、その程度はSHRがWKYに比較して大であった(412±26 vs 162±14 nM, p<0.05)。CF6によるCa influxとAngII依存性Ca濃度上昇の増強作用はc-Src阻害薬PP1の前投与により消失した。【結論】CF6はVSMC表面のATP合成酵素β-subunitと結合し、細胞内へのHのinfluxを亢進させた。CF6はc-Srcの活性化を介して、Ca influxとAngII依存性Ca濃度上昇の亢進作用を示した。これらの反応はSHRで亢進しており、CF6の高血圧への関与が示唆された。

BP-13 Histidineは中枢H_3受容体刺激による交感神経活動抑制を介して自然発症高血圧ラットの血圧を低下させる

鳥羽 裕恵[1]、中森 亜矢子[1]、田中 良実[1]、雪矢 良輔[1]、小原 幸[1]、
針生 仁[2]、時高 正明[2]、中田 徹男[1]
[1]京都薬科大学 臨床薬理学教室、[2]株式会社シマヤ 商品開発部

【目的】Histidineは鰹などの回遊魚の骨格筋に多く含まれるジペプチドで、近年、その降圧効果が示唆されている。本検討では自然発症高血圧ラット(SHR)を用いて、histidineによる降圧効果について、中枢H_3受容体と交感神経の関与を含め検討した。【方法】実験には9週齢のSHRを用いた。Histidine (100 mg/kg) はすべてgavage法で投与した。<実験1>Histidineの急性投与後12時間の平均動脈圧(MAP)の変化を大腿動脈に挿入したカニューレから覚醒下観血的に測定した。<実験2>1日2回、5週間、histidineを慢性投与し、以下の検討を行った。投与期間中1週毎に、代謝ケージによる24時間蓄尿から尿中カテコラミン排泄量とtail-cuff法にて収縮期血圧(SBP)を測定した。5週間後、histidine経口投与後12時間の覚醒下MAPの変化と、H_3受容体拮抗薬thioperamide脳室内投与後の麻酔下MAPへの影響を持続的に記録した。<実験3>Histidineを1日1回、2週間慢性投与した後の胸部大動脈組織におけるACE mRNA発現をRT-PCR法にて検討した。【成績】<実験1>Histidine急性経口投与後、SHRのMAPは投与前に比べ有意に低下し、12時間後には投与前値に戻った。<実験2>Histidine投与3週目よりSBPの上昇が抑制され、1週目と3週目で尿中カテコラミン排泄量が低下した。Histidine慢性投与群ではhistidine投与後12時間以上、降圧効果が持続した。一方、無処置のSHRの麻酔下MAPにthioperamideは影響を与えなかったが、histidine慢性投与群ではthioperamideの脳室内投与によりhistidineの降圧効果は消失し、昇圧した。<実験3>Histidine投与群の胸部大動脈組織ではACEのmRNA発現が抑制された。【結論】Histidineの急性および慢性経口投与は中枢H_3受容体を介し交換神経活動を抑制することで、降圧効果を発揮した。さらに、血管壁における組織ACE発現抑制による血管保護効果も示唆された。

BP-14 脳卒中易発症性自然発症高血圧ラットにおける脳内酸化ストレスとアンジオテンシンIIタイプ1受容体拮抗薬オルメサルタンによる治療効果：In vivo ESR法の応用

荒木 周一郎[1]、廣岡 良隆[1]、野副 純世[1]、古閑 靖章[1]、岸 拓也[1]、
安川 圭司[2]、内海 英雄[2]、砂川 賢二[1]
[1]九州大学 循環器内科、[2]九州大学薬学部 機能分子解析学

【目的】高血圧の中枢性機序に脳内酸化ストレスが深く関与していることを、我々は示してきた。アンジオテンシンIIタイプ1(AT1)受容体刺激は活性酸素産生を増加することが示唆されている。しかし、脳内活性酸素の評価、特に*in vivo*測定はこれまで困難であった。従って、本研究の目的は、生体電子スピン共鳴／スピンプローブ法 (*in vivo*ESR) を用い、非侵襲的に高血圧モデル動物である脳卒中易発症性自然発症高血圧ラット(SHRSP)及び週齢の同じ正常血圧コントロールであるWistar-Kyoto ラット (WKY) の脳内活性酸素産生を測定する手法を確立し、さらにAT1受容体拮抗薬であるオルメサルタン メドキソミル (Olm) による降圧治療の脳内活性酸素産生に対する効果を検討することであった。
【方法】12週齢のSHRSPを2群に分け、Olm(10 mg/kg/day) 又は、ヒドララジン(Hyd, 20 mg/kg/day) ／ヒドロクロロチアジド (Hct, 4.5 mg/kg/day) (n = 5 for each) をそれぞれ30日間投与した。*in vivo* ESRは、低周波数 (300 MHz) のESR装置、及びスピンプローブとして血液脳関門通過性のmethylcarbonyl-PROXYL (MC-P) を用いて行った。尾静脈内投与後、脳に集積したMC-Pの、内因性フリーラジカルとの反応によるスピンの消失を、ESRシグナル強度の減衰率(/min) として測定した。
【結果】Olm及びHyd/HCT投与により同等の降圧効果 (151±8 mm Hg [Olm] vs. 156±13 mm Hg, [Hyd/HCT], NS) が認められたが、心拍数、及び24時間尿中ノルエピネフリン排泄量はHyd/HCT群においてのみ増加した。SHRSPの脳におけるESRシグナル減衰率はWKYと比し増加しており(0.121±0.010 /min vs. 0.098±0.011 /min, p< 0.01, n = 6 for each, SHRSP vs. WKY, respectively)、この増加は、ハイドロキシラジカルスカベンジャーであるdimethylthiourea、及び、NAD (P)H オキシダーゼ阻害薬であるapocyninの投与により、抑制された。ESRシグナル減衰率の増加はOlm群において有意に抑制された (0.102±0.004 /min vs. 0.120±0.008 /min, p<0.01, post- vs. pre-treatment, respectively) が、Hyd／Hct群では、有意な変化を認めなかった。
【結論】以上の成績は、*in vivo* ESRによるSHRSPの脳内活性酸素産生の測定が可能であること、さらに、AT1受容体拮抗薬であるOlmが、血圧降下作用に加え、その増加した脳内活性酸素産生の抑制効果を有していることを示唆する。

BP-15 インスリン抵抗性と食塩感受性高血圧における吻側延髄腹外側野のKAT-1遺伝子の役割

伊藤 哲[1]、小松 一俊[1]、飯塚 陽子[2]、後藤田 貴也[3]、矢島 愛治[1]、
金井 孝司[1]、塚本 一義[1]、藤田 敏郎[3]、平山 篤志[1]
[1]日本大学医学部 内科学講座 循環器内科部門、[2]東京大学 糖尿病代謝内科、[3]東京大学 腎臓内分泌内科

【目的】kynureninne amionotransferase-1 (KAT-1) は、kynurenineから内因性広範囲興奮性アミノ酸拮抗物質であるkynurenic acidへの変換酵素である。我々は、既にメタボリックシンドロームのモデルである自然発症高血圧ラット (SHR) のインスリン抵抗性そして高血圧発症機序に吻側延髄腹外側野 (RVLM) におけるKAT-1のミスセンス変異が関与している事を報告している。一方、最近メタボリックシンドローム・インスリン抵抗性高血圧と食塩感受性高血圧との関係が注目されている。そこで今回我々は、食塩感受性高血圧とRVLMにおけるKAT-1の役割に関して検討した。【方法】1) 雄性Wistar Kyoto ラット (WKY) にテレメトリーシステムを挿入し、ハロセン麻酔下に両側RVLMにKAT-1遺伝子アンチセンスを含む組み換えアデノウイルス (KAT-1 antisense) とLacZ遺伝子を含むAdLacZを微量注入した。さらに別群には、テレメトリーシステム挿入2週間前より8%高塩食負荷を開始して、導入以後も継続した。【成績】1) 導入後、KAT-1antisense群においてのみRVLMに局在してKAT-1活性の低下を認めた。しかしながらKAT-1antisense群の覚醒自由行動下の血圧及び心拍数は、AdLacZ群と比較して有意な変動は全経過中認めなかった。自由行動下の交感神経活動も有意な変化を認めなかった。2) 一方高塩食群においては、KAT-1antisense群にて、導入後にAdLacZ群と比較して有意な血圧と心拍数増加に加えて交感神経活動の増加を認めた。【結論】WKYのRVLMへのKAT-1遺伝子アンチセンスの導入は、RVLMに限局してKAT-1活性の低下を認めた。しかしながら交感神経活動は、有意な変化を認めず血圧、心拍数には変化を生じなかった。一方、高塩食群においては、KAT-1antisense群にて有意な交感神経活動の増加に伴い血圧、心拍数の上昇を認めた。以上より、RVLMにおけるKAT-1活性の低下と、食塩負荷の組み合わせは、RVLMにおける興奮性アミノ酸入力の不均衡をもたらし、交感神経活動を亢進させ食塩感受性高血圧を引き起こす事が示唆された。一方で、RVLMに局在したKAT-1活性の低下のみでは、交感神経活動の亢進は認められなかった。食塩負荷は、視床下部室傍核よりRVLMを介する興奮性交感神経作動性入力を亢進させる作用を有しており、上位中枢よりの刺激の亢進とRVLMにおけるKAT-1活性の低下による興奮性アミノ酸入力の不均衡が交感神経活動亢進を来した事が予想される。このことからも、食塩感受性と中枢特にRVLMにおけるKAT-1活性の低下による興奮性アミノ酸入力の不均衡が密接に関係し、食塩負荷による交感神経活動亢進を起こしさらにインスリン抵抗性を惹起する事の可能性が示唆された。

BP-16 食後高血糖を想定した急性的な高血糖および高血中インスリン状態における神経性血圧調節機能の異常

座間味 義人、岩谷 有希子、小山 敏広、藪前 奈々、川崎 博己
岡山大学大学院医歯薬学総合研究科 臨床薬学

【目的】近年、増加している糖尿病発症以前の境界型患者に食後の高血糖を抑えるαグルコシダーゼ阻害薬を投与すると高血圧の発症が有意に抑制されたという報告から、食後高血糖が糖尿病で見られる高血圧の原因の一つである可能性が示唆されている。我々はこれまでグルコースを持続注入することにより食後高血糖を想定した高インスリン血症を伴った急性高血糖状態を作製し、この条件下では交感神経機能の亢進と血管拡張性calcitonin gene-related peptide (CGRP) 神経機能の低下を起こすことを明らかにした。そこで本研究では、神経性による血圧反応に及ぼす高血糖および高血中インスリンの各単独における影響をin vivo系において検討した。【方法】pentobarbital麻酔下に脊髄穿刺ラット (Wistar系雄性) を作成した。オクトレオチドを前投与し内因性インスリン分泌を抑制した状態で頸静脈よりグルコースを持続注入し、人工的に高血糖状態にし、脊髄電気刺激(SCS) およびnoradrenalineの静注による昇圧反応を観察した。また、hexamethoniumで自律神経節を遮断し、α1受容体作動薬methoxamineで平均血圧を120 mmHg程度に上昇させた状態でSCSおよびCGRPによる降圧反応を観察した。一方、インスリンと正常血糖を保つためにグルコースを同時に持続注入して作製した高血中インスリンの条件下でも同様に血圧反応性の変化を検討した。【結果および考察】オクトレオチド前処置後、グルコース注入を行うと血糖値は上昇したが、グルコース刺激に対する血清インスリン値の上昇は抑制された。この高血糖条件下におけるSCSによる交感神経性昇圧反応は容量のコントロールとして持続注入したsaline群と比較すると有意に大きな値を示したが、noradrenalineによる昇圧反応では有意な差は認められなかった。またCGRP神経性降圧反応およびCGRPによる降圧反応はsaline群とほぼ同じ値を示した。一方、インスリンを持続注入して作製した高血中インスリンの条件下ではSCSによる交感神経性昇圧反応はsaline群と比べて有意に大きな値を示し、CGRP神経性降圧反応は有意に小さな値を示した。また高血糖条件下と同様にnoradrenalineによる昇圧反応およびCGRPによる降圧反応には有意な差は認められなかった。【結論】以上の結果、急性的な高血糖は交感神経を亢進し、高インスリンはCGRP神経機能を低下させるという知見が得られた。したがって、耐糖能異常患者や糖尿病患者の食後に見られる一時的な高血糖とそれに伴うインスリン過剰分泌により起こる血中インスリン濃度上昇が交感神経およびCGRP神経による血管緊張度調節系の異常を引き起こし、これが高血圧発症の要因になっている可能性が示唆される。

CP-48 高血圧患者におけるアゼルニジピンの自律神経活動に及ぼす影響

北村　哲也[1]、伊藤　正明[2]
[1]鈴鹿中央総合病院 循環器科、[2]三重大学大学院医学系研究科 循環器内科学

【目的】ジヒドロピリジン(DHP)系Ca拮抗薬は高血圧症患者に対して、確実な降圧効果が期待できることから我が国でも広く使用されてきたが、特に短時間作用型のCa拮抗薬においては降圧にともない交感神経系が刺激されることが指摘されている。高血圧患者における交感神経系の活性は、臨床上の大きな問題点であるが、第三世代DHP系Ca拮抗薬と言われるアムロジピンであっても、交感神経系が亢進し、心拍数が増加することが報告されている。長時間作用型DHP系Ca拮抗薬であるアゼルニジピンはアムロジピンと同等の降圧効果を有しながら、心拍数は増加させないと報告されており交感神経系への影響が少ないと期待されている薬剤である。今回我々は、アムロジピンにて加療中の本態性高血圧患者を対象に、アゼルニジピンの降圧効果と、自律神経活動に及ぼす影響について検討した。【方法】対象はアムロジピン5mg/日で6ヶ月以上治療中の本態性高血圧患者22例(男性17例、女性5例、平均年齢69±8歳)。アムロジピン投与中と、アムロジピンからアゼルニジピン16mg/日に切り替えた6ヶ月後の時点で、血圧・心拍数、Holter心電図を用いた自律神経活動の指標、酸化ストレスマーカー等を測定して比較検討した。【成績】アゼルニジピンへの切り替えで、血圧値は収縮期血圧が145±15から137±16mmHg、拡張期血圧が82±8から78±10mmHgまで有意に低下した(p<0.05)。心拍数は70±7から64±5bpmに有意に低下した(p<0.05)。血中カテコラミン濃度(アドレナリン、ノルアドレナリン、ドーパミン)、高感度CRP、尿中イソプラスタン、尿中8-OHdG(8-ヒドロキシデオキシグアノシン)に変化はなかった。24時間の平均でみた心拍変動スペクトル解析では、副交感神経系活動指標のhigh frequency(HF) power、HF/TP比や、交感神経活動指標のlow frequency(LF) powerは変化なかったが、交感・副交感神経系活動のバランス指標となるLF/HF比は、3.5±2.2から3.1±1.9に有意に低下した(p<0.05)。またultra low frequency(ULF) powerは約30%増加した(p<0.05)。【結論】アゼルニジピンは、アムロジピンより降圧効果が高く、心拍数を有意に減少させた。また、LF/HF比の有意な低下を認めたことから、アゼルニジピンが交感神経活動を抑える点で優れている可能性があることが示唆された。

CP-49 2つのCaチャネルブロッカー、シルニジピンとアゼルニジピンの家庭心拍数に対する影響

山岸　俊夫
東北公済病院 内科

【目的】Caチャネルブロッカーのうち、シルニジピンとアゼルニジピンは、降圧に伴う反射性の心拍数の増加が少ない、あるいは低下させる降圧薬として知られている。しかしその機序には差異があり、L型Caチャネルの抑制による降圧に加え、シルニジピンでは、交感神経のN型Caチャネルの抑制があり、またアゼルニジピンでは、圧受容体感受性(BRS)の改善により、心拍数を低下させるとされている。今回、家庭血圧計を用いて家庭高血圧と家庭心拍数に対する作用について検討したので報告する。
【方法】対象は外来通院中の本態性高血圧患者66名(年齢58±10歳、男32、女34、早朝家庭収縮期血圧135mmHgまたは拡張期85mmHg以上)に対し、シルニジピン(C)10mg(16名)、20mg(21名)あるいはアゼルニジピン(A)8mg(10名)、16mg(19名)を1日1回朝食後に投与した。家庭血圧と家庭心拍数は、本学会の指針のとおりに上腕家庭血圧測定装置を用いて測定した。投与前および投与開始から12週間後の外来血圧、早朝家庭血圧および心拍数(前後5日の平均)を比較し(結果は平均±標準偏差で表記)、p<0.05を有意とした。
【成績】投与前の早朝家庭血圧および家庭心拍数はC群148.9±10.9/93.2±6.5mmHg、70.4±18.6拍／分、A群152.1±12.4/93.8±10.7mmHg、72.4±8.0拍／分で、両群で差はなかった。降圧度(収縮期/拡張期)はベースラインと比較して、C群では、10mgで-15.3±8.4/-9.0±6.4mmHg、20mgで-17.8±10.0/-11.0±6.4mmHgに対し、A群では、8mgで-12.6±7.8/-8.3±7.6 mmHg、16mgで-23.6±10.2/-15.5±12.3mmHgであり、両薬剤とも投与前に比し有意に、また用量依存的に血圧を低下させた。しかし家庭心拍数(拍/分)はベースラインと比較して、A群では、8mgで-2.1±2.2、16mgで-7.5±7.9と有意に、用量依存的に低下していたが、C群では、10mgで-0.8±5.4と有意な変化はなく、20mgで-6.4±6.5でのみ有意に低下していた。また心拍数の低下した患者の割合は、A群8mgでは80%、16mgでは90%であり、C群10mgでは69%で、20mgでは81%であった。常用量での比較では、A16mgがC10mgに比して有意に家庭心拍数を低下させていたが、外来心拍数では差はなかった。
【結論】家庭心拍数に対して、アゼルニジピンは低用量から心拍数低下作用があり、またシルニジピンの心拍数低下作用はより高用量で発現した。両Caチャネルブロッカーにおいて心拍数低下作用機序の異なる可能性が、家庭心拍数低下パターンからも示された。

CP-50 本態性高血圧患者に対するアゼルニジピン内服治療は交感神経活動抑制および動脈圧受容器反射改善作用を有する

今野　里美、廣岡　良隆、岸　拓弥、砂川　賢二
九州大学大学院医学研究院 循環器内科学

【目的】長時間作用型のL type Caチャンネル遮断薬で最も新しいアゼルニジピンは、従来のジヒドロピリジン系Caチャンネル遮断薬と異なり、臨床使用において心拍数を上昇させないという報告が散見される。また、動物実験では、アゼルニジピンに中枢性循環調節機序を介した交感神経活動抑制作用があることを、これまで我々のグループを中心に報告してきた。しかしながら、ヒトでの高血圧治療において、アゼルニジピンに交感神経活動抑制作用があるかどうか、また、高血圧患者では障害されている動脈圧受容器反射を改善させる作用があるかどうかについては明らかではない。そこで本研究の目的は、本態性高血圧患者に対するアゼルニジピンによる治療において、交感神経活動抑制作用および動脈圧受容器反射改善作用があるかどうかを明らかにすることであった。【方法】10名の本態性高血圧患者に対し、JSH2004に準じてアゼルニジピン単独による高血圧治療を3ヶ月行い、5名がアゼルニジピン8mgで、5名がアゼルニジピン16mgで良好な降圧が得られた。収縮期血圧および心拍変動周波数解析を治療前後で行い、交感神経活動の指標として収縮期血圧変動総周波数パワーにおける低周波成分の割合(LFnuSBP)を、副交感神経活動の指標として心拍変動総周波数パワーにおける高周波成分の割合(HFnuRRI)を用いた。動脈圧受容器反射は、収縮期血圧および心拍数の変動からsequence methodを用いてbaroreflex sensitivity(BRS)を測定した。【成績】収縮期/拡張期血圧は、アゼルニジピン8mg群において156±12/98±6mmHg→131±4/83±6mmHg、16mg群において160±8/100±5mmHg→118±8/79±6mmHgと有意に低下を認めた。両群ともに心拍数は低下する傾向にはあったが有意な低下は認められなかった。交感神経活動の指標として用いたLFnuSBPは、アゼルニジピン8mg群において56±4%→50±3%、16mg群において62±5%→51±4%と有意に低下を認めたが、副交感神経活動の指標として用いたHFnuRRIは両群ともに有意な変化は認められなかった。BRSは、アゼルニジピン8mg群においては12.8±4.2ms/mmHg→15.6±8.3ms/mmHgと有意な改善は認められなかったが、16mg群において13.8±2.8ms/mmHg→19.8±4.1ms/mmHgと有意な改善を認めた。【結論】ヒト本態性高血圧患者において、3ヶ月間のアゼルニジピン内服により、用量依存性に交感神経活動抑制および動脈圧受容器反射改善作用を有する可能性が示唆された。この機序として、単なる緩徐な降圧によるものだけではなく、中枢性循環調節、特に交感神経活動中枢への直接抑制作用が関与している可能性がある。

CP-51 軽症～中等症の高血圧患者の血圧、脈拍及び自律神経機能に対するcilnidipineの長期効果についての検討

甲斐　達也[1]、原　秀憲[2]、葛本　佳正[2]、金政　健[1]
[1]近畿大学 高血圧・老年内科、[2]近畿大学 神経内科

【目的】我々は、これまでにcilnidipineの3ヶ月投与が、軽症～中等症の高血圧患者の血圧、脈拍及び交感神経機能を改善することを報告している。今回、我々はその効果が6ヶ月間の投与においても維持されているかについて検討を行った。【方法】15名の軽症～中等症の高血圧患者(男性6名、女性9名、平均年齢61歳)を対照とした。各患者に対し、収縮期及び拡張期血圧、心拍数、Valsalva maneuverのIIL相後期及びIV相での連続測定血圧、Valsalva指数,及び呼吸心拍変動の測定とHead-up tilt testを行った。その後各患者にcilnidipine 10mg/dayを6ヶ月間経口投与し、cilnidipine投与3ヵ月後と6ヵ月後に投与前と同じ項目の検査を施行し検討を行った。【成績】cilnidipineの投与により、6ヵ月後には収縮期血圧は151±4mmHg(Mean±SE)から134±4mmHgへと有意に低下し、拡張期血圧も84±3mmHgから74±4mmHgへと有意に低下した。心拍数は、cilnidipine投与前後で有意な変化は認めなかった。Valsalva maneuverのIIL相後期とIV相の連続測定血圧は、cilnidipine投与によりそれぞれ14.9±4.13mmHgから2.5±3.6mmHg、20.7±2.9mmHgから9.5±1.8mmHgへと有意に改善した。一方、Valsalva指数と呼吸心拍変動は、cilnidipine投与前後で有意差は認めず、head-up tilt testにおいてもcilnidipine投与前後ともに起立性低血圧は認めなかった。投与3ヶ月後と6ヵ月後比較では、IV相のみ有意な差を認めたものの、他の測定項目は有意な差を認めなかった。【結論】今回の研究において、L型及びN型カルシウムチャネルブロッカーであるcilnidipineの投与により、脈拍数に有意な変化を与えることなく血圧の有意な低下と交感神経α及びβ機能の改善が認められ、その効果は6ヵ月後においても持続していた。但し、交感神経β機能の改善効果は、長期には減少すると考えられた。

Vol 116, No 16, October 16, 2007
ISSN 0009-7322
http://circ.ahajournals.org

American Heart Association®
Learn and Live℠

SUPPLEMENT TO

Circulation

JOURNAL OF THE AMERICAN HEART ASSOCIATION

Abstracts from

scientific sessions 2007

Pre-Sessions Symposia: November 3
Exhibits: November 4–6
Sessions: November 4–7
Orlando, Florida
scientificsessions.org

basic science
clinical science
population science
translational science

Named and Invited Lectures 2007

2007 Russell Ross Memorial Lectureship in Vascular Biology • 2007 George L. Duff Memorial Lecture • 2007 Sol Sherry Distinguished Lecture in Thrombosis • 2007 Thomas W. Smith Memorial Lecture • 2007 George E. Brown Memorial Lecture • 2007 Dickinson W. Richards Memorial Lecture • 2007 Katharine A. Lembright Award & Lecture • 2007 William W. L. Glenn Lecture • 2007 William J. Rashkind Memorial Lecture • 2007 T. Duckett Jones Memorial Lecture • 2007 Charles T. Dotter Memorial Lecture • 2007 Laennec Clinician/Educator Lecture • 2007 James B. Herrick Award and Lecture • 2007 Ancel Keys Memorial Lecture • 2007 Donald Seldin Lecture • 2007 Robert Levy Memorial Lecture • 2007 Stroke Council Award and Lecture • 2007 Distinguished Scientist Lecture • 2007 Paul Dudley White Lecture

Council Early Career Investigator Awards 2007

Louis N. and Arnold M. Katz Basic Science Research Prize for Young Investigators • Melvin L. Marcus Young Investigator Awards in Cardiovascular Science • Cournand and Comroe Young Investigator Prize in Cardiopulmonary and Critical Care • Melvin Judkins Young Investigator Award in Cardiovascular Radiology • Vivien Thomas Young Investigator Award • Martha N. Hill New Investigator Award • Elizabeth Barrett-Connor Research Award in Epidemiology and Prevention for Investigators in Training • Samuel A. Levine Young Clinical Investigator Award • Laennec Young Clinician Award • NPAM New Investigator Award

Abstracts From the Scientific Sessions 2007

rejuvenation of CSN in cardiac hypertrophy. **Methods and Results:** (1) RV hypertrophy was produced by consistent hypoxia (10% O_2) in C57/BL6 mice. RV pressure increased to 47 mmHg, and RV/ (body weight) ratio increased by 1.6 fold. (2) Nerve growth factor protein was augmented in hypertrophic RV, but was unchanged in LV. (3) Double-transgenic mice, which specifically express eGFP (enhanced green fluorescent protein) in the sympathetic neurons, was generated by crossing dopamine β-hydroxylase (DBH)-Cre mice with Floxed-eGFP mice. The eGFP-positive CSN were markedly increased in hypertrophic RV, but not in LV. Nerve density, quantitated by immunostained-area with eGFP and GAP43 (growth-associated corn marker), increased by 8.1 and 9.3 fold, respectively, in RV, but not in LV. (4) Catecholamine content was attenuated in RV. (5) Western blot revealed that tyrosine hydroxylase was markedly down-regulated in RV. (6) Immunostaining clearly demonstrated that the immature neuron markers, PSA-NCAM (highly polysialylated neural cell adhesion molecule) and Ulip-1 (Unc-33-like phosphoprotein 1), were expressed in CSN in hypertrophic RV and stellate ganglia. Basic helix-loop-helix transcription factor, Mash-1 (mammalian achaete-scute complex homolog 1) was strongly expressed in the stellate ganglia. (7) Immature neuron marker-immunopositive cells in stellate ganglia had a markedly decreased TH expression. **Conclusion:** The rejuvenated CSN showed various immature and fetal neuron marker genes at not only the peripheral axons but also the cellular bodies at the stellate ganglia. Rejuvenation of CSN might be critically involved in the alteration of sympathetic neuronal function in cardiac hypertrophy, including depressed norepinephrine synthesis and hyperinnervation.

1373

High Salt Diet Exacerbates Hypertension via Increased Oxidative Stress in the Rostral Ventrolateral Medulla and Sympathetic Hyperactivity in Spontaneously Hypertensive Rats

Yasuaki Koga, Yoshitaka Hirooka, Shuichiro Araki, Masatsugu Nozoe, Takuya Kishi, Kenji Sunagawa; Dept of Cardiovascular Medicine, Kyushu Univ Graduate Sch of Med Sciences, Fukuoka, Japan

Background: A high salt diet (HS) causes sympathetic hyperactivity and increases resting blood pressure (BP) in spontaneously hypertensive rats (SHR). Reactive oxygen species (ROS) in the rostral ventrolateral medulla (RVLM) are increased in hypertensive rats and AT$_1$ receptor stimulation activates ROS generation. We examined whether HS increases ROS in the RVLM of SHR and, if so, whether this increase in ROS generation is caused by central angiotensin II activation via NAD(P)H oxidase. ***Methods and Results:*** Male 6-week-old SHR and Wistar-Kyoto rats (WKY) were fed an HS (8%NaCl) or regular salt diet (0.5%NaCl; RS) for 6 weeks. BP was measured by the tail-cuff method. At 12 weeks of age, systolic BP was significantly higher in HS-SHR than in RS-SHR from 8 weeks of age on (214±4 mmHg vs 172±4 mmHg, n=8, $P<0.05$). Urinary norepinephrine excretion was significantly higher in HS-SHR than in RS-SHR at 12 weeks of age (2.09±0.10 μg/day vs 1.47±0.05 μg/day, n=5, $P<0.05$). ROS levels in the RVLM were evaluated by measuring the levels of thiobarbituric acid-reactive substances (TBARs). TBARs levels were significantly higher in the RVLM of HS-SHR than RS-SHR (9.9±0.5 μmol/g wet wt vs 8.1±0.6 μmol/g wet wt, n=5, $P<0.05$). To confirm the role of ROS in the RVLM in BP regulation, tempol was microinjected bilaterally into the RVLM of 12-week-old SHR. Microinjection of tempol into the RVLM induced a significantly greater BP depression in HS-SHR than in RS-SHR. Intravenous hexamethonium induced a significantly greater decrease in BP in HS-SHR than in RS-SHR, indicating enhanced sympathetic outflow in HS-SHR. Angiotensin II type1 receptor (AT$_1$R) expression in the RVLM was measured by Western blotting and NAD(P)H-dependent superoxide production in the RVLM was measured by lucigenin luminescence. AT$_1$R expression in the RVLM was significantly higher in HS-SHR than RS-SHR (5.1±0.5 vs 3.4±0.3, n=6, $P<0.05$). NAD(P)H-dependent superoxide production was higher in the RVLM from HS-SHR than RS-SHR. ***Conclusions:*** These results suggest that SHR on an HS diet have significantly increased ROS generation in the RVLM resulting in further BP elevation by activation of the sympathetic nervous system. Increased ROS generation is probably due to NAD(P)H oxidase activation via central angiotensin system.

1374

Sympathetic Overactivity Precedes Metabolic Dysfunction In Insulin Resistant Mice

Katia De Angelis, Sao JudasTadeu Univ; Sao Paulo, Brazil; Danielle Senador, Wright State Univ, Boonshoft Sch of Medicine, Dayton, OH; MC Irigoyen, Heart Institute (InCor), Sch of Medicine, Univ of Sao Paulo, Sao Paulo, Brazil; Mariana Morris, Wright State Univ, Boonshoft Sch of Medicine, Dayton, OH

The mechanisms that underlie the relationship between metabolic syndrome and cardiovascular dysfunction are unclear. The increasing incidence of diabetes and cardiovascular disease may be related to dietary changes, including consumption of high levels of fructose. The aim was to investigate the time course of the metabolic and cardiovascular alterations induced by fructose overload in the drinking water (100 g/L). C57/BL mice were divided into 3 groups: controls (C), 15 days-fructose (F15), and 60 days-fructose (F60). Mice were instrumented with radiotelemetric arterial catheters to light/dark pattern of systolic arterial pressure (SAP) and SAP variability measurement. Plasma glucose, lipids, insulin, leptin and glucose tolerance were also quantified. Fructose mice showed higher SAP at 15 and 60 days during both the light (F15: 123±2 and F60: 118±2 mmHg) and dark periods (F15: 136±4 and F60: 136±5 mmHg) as compared to controls (light: 111±2 and dark: 117±2 mmHg). SAP variance (VAR) was unchanged at F15, but was increased at F60 (light: 18±3 and dark: 37±7 ms^2) in relation to C group (light: 6±1 and dark: 14±1ms^2). The low frequency component (LF) of SAP variability was enhanced in the light and dark periods in fructose groups as compared to controls. Metabolic parameters were unchanged at day 15 day. After 60 days of fructose, there were significant increases in plasma glucose (26%), cholesterol (44%), triglycerides (22%), insulin (95%), leptin (63%) as well as glucose intolerance. The LF component of SAP VAR was positively correlated with SAP and VAR after 15 (r=0.84 and r=0.95) and 60 days (r=0.87 and r=0.92). The plasma leptin was associated with body weight and the glucose tolerance (AUC) after 15 (r=0.85 and r=0.8) and 60 days (r=0.8 and r=0.87) as well as with plasma insulin (r=0.8) after 60 days. The increases in plasma insulin and leptin indicate that this mouse model of fructose loading in the drinking water is similar to the human condition of type2 diabetes. The results also show that increased sympathetic activity preceded metabolic dysfunction in fructose fed mice, suggesting that sympathetic overactivity may be a key mechanism underling the cluster of cardiovascular and metabolic symptoms associated with metabolic syndrome.

1375

Brain Renin Angiotensin Blockade Attenuates Cytokines and Oxidative Stress in the Paraventricular Nucleus of Hypothalamus and Decreases Sympathoexcitation in Heart Failure Rats

Ying Ma, Yu-Ming Kang*, Zhi-Ming Yang, Shanxi Med Univ, Taiyuan, China; Joseph Francis*, Louisiana State Univ, Baton Rouge, LA

Introduction: Neurohumoral mechanisms play an important role in the pathophysiology of congestive heart failure (HF). Recent studies suggest that the brain renin angiotensin system (RAS) plays an important role in regulating body fluids and sympathetic drive in HF. In addition, it has been shown that there is cross talk between cytokines and RAS in cardiovascular disease. In this study we determined whether blockade of brain RAS attenuate inflammatory cytokines and oxidative stress in HF rats. **Methods and Results:** Adult male Sprague-Dawley rats were implanted with intracerebroventricular (ICV) cannulae and subjected to coronary artery ligation to induce HF and confirmed by echocardiography. Rats were treated with an angiotensin type 1 receptors (AT1-R) antagonist losartan (LOS, 20 μg/hr, ICV) or vehicle (VEH) for 4 weeks. At the end of the study, left ventricular (LV) function was measured by echocardiography and rats were sacrificed, and brain and plasma samples were collected for measurements of cytokines and superoxide using immunohistochemistry, Western blot and real time RT-PCR. HF rats induced significant increases in Nuclear Factor-kappaB (NF-κB) p50-positive neurons and activated microglia in the paraventricular nucleus (PVN) of hypothalamus, and TNF-α, IL-1β, IL-6 and NF-κB p50 in hypothalamus when compared with sham rats. These animals also had increased staining for dihydroethidium (DHE) and plasma levels of norepinephrine (NE), an indirect indicator of sympathetic activity. In contrast, ICV treatment with LOS attenuated cytokine expression and oxidative stress in the PVN and hypothalamus when compared with VEH treated HF rats. ICV treatment with LOS also reduced plasma NE levels, and proinflammatory cytokine, heart weight to body weight ratio with decreased LV end-diastolic pressure. **Conclusions:** These findings suggest the cross talk between the cytokines and renin angiotensin system within the brain contribute to sympatho-excitation in HF.

Group	plasma IL-1β (pg/ml)	plasma NE (pg/ml)	hypothalamus TNF-α (pg/mg protein)	LVEDP (mmHg)	LVEF (%)	COX-2 in PVN (intensity of fluorescence)	p50 positive PVN neurons (number of cells)	DHE in PVN (intensity of fluorescence)	p50 protein in hypothalamus (densitometric units/μg protein)
HF+ICV VEH (n=12)	130.6 ± 10.4#	258.3 ± 12.6#	7.0 ± 0.8#	20.3 ± 1.3#	36.2 ± 4.1#	52.6 ± 5.9#	68.2 ± 6.1#	94.6 ± 7.9#	90.2 ± 8.4#
HF+ICV LOS (n=12)	89.2 ± 8.1*#	219.5 ± 7.2*#	5.2 ± 0.6*#	11.4 ± 1.1*#	41.6 ± 5.2#	31.8 ± 4.0*#	41.3 ± 4.0*#	69.2 ± 6.4*#	64.8 ± 4.2*#
SHAM+ICV LOS (n=12)	59.1 ± 3.6	172.8 ± 8.4	3.1 ± 0.5	3.9 ± 0.9	84.1 ± 6.4	15.6 ± 3.9	14.6 ± 3.1	35.1 ± 4.0	29.6 ± 4.6
SHAM+ICV VEH (n=12)	62.8 ± 4.2	179.1 ± 10.5	3.5 ± 0.6	4.5 ± 1.0	81.5 ± 5.5	18.1 ± 4.5	20.3 ± 3.4	41.5 ± 4.9	36.4 ± 4.5

1376

Destruction Of Cardiac Sympathetic Afferents Normalizes Sympathoexcitation In Chronic Heart Failure

Wei-Zhong Wang, Lie Gao, Yan-Xia Pan, Irving H Zucker, Wei Wang; Dept of Physiology, Nebraska Med Cntr, Omaha, NE

The enhanced cardiac "sympathetic afferent" reflex has been demonstrated to contribute to increased sympathetic outflow in chronic heart failure (CHF). This is associated with increased angiotensin II in the central nervous system. The rostral ventrolateral medulla (RVLM) has been recognized as a critical area involved in sympathetic outflow. Therefore, the objective of this study was to assess whether inhibition of cardiac sympathetic afferent input decreases sympathetic activity, and if so, whether AT1 receptor mechanisms in the RVLM contribute to this response. The cardiac sympathetic afferents were destroyed by left ventricular epicardial application of resiniferatoxin (RTX, 200 mg) while infraction or sham surgery was performed. The rats were allowed to recover 6 to 8 weeks after surgery. A total of 47 rats were divided into four groups: sham, sham + RTX, CHF, and CHF + RTX. The Table shows the expression of AT1 receptor protein in the RVLM, the baseline RSNA, and the responses of blood pressure and RSNA to RVLM injection of the AT1 receptor antagonist losartan in the four groups. These results indicate that chronic blockade of the cardiac sympathetic afferent reflex by destruction of cardiac sympathetic afferents normalizes the sympatho-excitation and downregulates the RVLM AT1 receptor in the CHF state, suggesting that tonic cardiac sympathetic afferent input contributes to increased sympathetic activity through the RVLM AT1 receptor mechanism in CHF.

	Sham	Sham + RTX	CHF	CHF + RTX
AT1 protein (Arbitrary units)	1.0 ±0.2(5)	0.8 ±0.2(5)	1.9 ±0.3*(7)	1.2 ±0.2†(6)
Basal RSNA (% of max)	45.4 ±5.3(4)	41.4 ±5.8(5)	68.3 ±7.4*(8)	51.1 ±6.2†(7)
ΔMAP (mmHg) by losartan	2.7 ±1.4(4)	2.1 ±2.1(5)	-8.3 ±1.2*(8)	-2.5 ±2.4†(7)
ΔRSNA (%) by losartan	5.3 ±9.3(4)	5.1 ±3.6(5)	-26.4 ±5.8*(8)	-7.3 ±2.1† (7)

Calmodulin antagonist W-7 (10 pmol in 50 nL) into the RVLM decreased baseline RSNA, MAP and HR. Pretreatment with U73122, Calphostin, or W-7 in the RVLM partially blocked Ang II induced sympathoexcitation (U73122 ΔRSNA 29.2 ± 3.4%; Calphostin ΔRSNA 41.3 ± 3.5%; W-7 ΔRSNA 38.9 ± 3.5%) and pressor responses (U73122 ΔMAP: 6.5 ± 0.8 mmHg; Calphostin ΔMAP: 11.4 ± 1.5 mmHg; W-7 ΔMAP: 12.1 ± 1.6 mmHg). These results suggested that both PLC-PKC and PLC-CaMKII pathways exert a tonic effect in the maintenance of baseline sympathetic activity and these two pathways partially mediate the response to exogenous Ang II in the RVLM in normal rats. This pathway may play a role in sympatho-excitatory states such as hypertension and chronic heart failure state.

1382

AlbuBNP (Cardeva), a Novel Recombinant Human B-Type Natriuretic Peptide Serum Albumin Fusion Protein Has Prolonged Renal Enhancing Properties When Compared to Human BNP.

Horng H Chen, Fernando L Matrin, Alessandro Cataliotti, John A Schirger, John C Burnett; Mayo Clinic, Rochester, MN

BACKGROUND: AlbuBNP is a novel recombinant human BNP serum albumin fusion protein which possesses a significantly longer elimination half-life compared to BNP. To date, it remains unclear if this novel protein which represents a single molecule of BNP synthesized with the carrier protein albumin can enter the post glomerular/tubular system due to the fusion of BNP to albumin and mediate renal actions. We hypothesized that this fusion protein will have potent renal actions and possess prolonged renal hemodynamic enhancing and excretory properties based upon its unique structure as compared to native BNP. **METHODS:** We compared the cardiorenal and humoral actions of intravenous(IV) bolus of administration of AlbuBNP (Cardeva; CoGenesys; Rockville MD) (5 mg/kg, n=7) and Human BNP (Phoenix Pharmaceutical, Belmont CA) (25 μ g/Kg, n=5) in two groups of normal anesthetized dogs. * p<0.05 **RESULTS:** Single IV bolus of AlbuBNP resulted in a sustained increase in plasma cGMP (5±1 to 9±2 pmol/ml†) and urinary cGMP excretion (1136±113 to 2556±417 pmol/min*), markers of the biological activity of BNP, which remained elevated at the termination of the experiment at 270 minutes. In contrast, with human BNP, both plasma and urinary cGMP peaked at 30 minutes and returned to baseline by 150 minutes. In a similar fashion, there was a sustained increase in natriuresis (39±12 to 159±38 μEq/min*), diuresis (0.2±0.1 to 1.1±0.3 ml/min*), renal blood flow (220±22 to 301±33 ml/min*), and glomerular filtration rate (34±2 to 62±13 ml/min*) with AlbuBNP, while with human BNP, these renal effects peaked at 30 minutes and returned to baseline by 150 minutes. Furthermore, there was a gradual and sustained suppression of plasma aldosterone (7.8±2 to 3.6±1 ng/dL*) with AlbuBNP. Likewise, there was a more sustained reduction of cardiac filling pressures with AlbuBNP as compared to human BNP. **CONCLUSION:** We report for the first time that this newly developed BNP/albumin fusion protein has a more prolonged and sustained renal enhancing properties compared to human BNP. Thus, AlbuBNP (Cardeva) represents a novel long-acting renal enhancing and aldosterone suppressing drug which has therapeutic potential for the management of cardiovascular and renal diseases that should be defined in further studies.

1383

Noninvasive Transcutaneous Bionic Baroreflex System Prevents Severe Orthostatic Hypotension in Spinal Cord Injury

Masayoshi Yoshida, Akiko Chishaki, Satoshi Kimura, Makoto Andou, Takaki Tsutsumi, Yoshinori Murayama, Kenji Sunagawa; Kyushu Univ Graduated Sch, Fukuoka, Japan

Background: Central baroreflex failure in spinal cord injuries results in serious orthostatic hypotension. Although various interventions such as salt loading and adrenergic agonists have been attempted to treat orthostatic hypotension, such interventions can neither restore nor reproduce the functioning of the native vasomotor center. We proposed a novel therapeutic strategy, i.e., an artificial feedback control system (bionic baroreflex system: BBS) capable of automatically regulating sympathetic vasomotor tone (Circulation 1999, 2002, 2004). Since somatic inputs are known to affect sympathetic drive in patients, we examined if the transcutaneous noninvasive electrical stimulation can be used to feedback control arterial pressure (AP) in spinal cord injury. **Methods and Results:** We identified skin regions (bilateral inguinal areas), windows of somato-splachnic reflex, capable of increasing AP in response to electrical stimulation. By a binary white noise approach with stimulation frequency 0-40-Hz (0.3 msec, 40 mA), we estimated the dynamic properties of the stimulation-AP responses (Fig. A) and, then, determined the transfer function required for the BBS. We examined the performance of BBS by imposing orthostatic stress (passive upright position). The orthostatic stress decreased AP to 45 mmHg (Fig. B). But the activation of BBS immediately restored AP to a prespecified level (65 mmHg) in ≤20 sec. The patient who had had serious orthostatic hypotension was totally free from any hypotensive symptoms. **Conclusion:** Transcutaneous bionic baroreflex system is noninvasive and capable of stabilizing AP in spinal cord injury with central baroreflex failure.

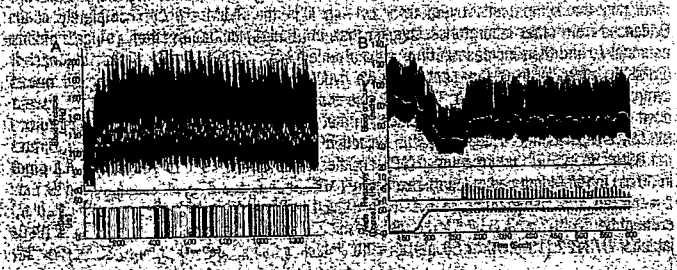

1384

Impaired Neurogenesis in the Rostral Ventrolateral Medulla Cause Hypertension in Stroke-prone Spontaneously Hypertensive Rats

Takuya Kishi, Yoshitaka Hirooka, Kenji Sunagawa; Kyushu Univ, Fukuoka, Japan

Background: Recent studies demonstrated that the neural progenitor cells that form neuroblasts were migrated directly to sites of brain injury in animal models of epilepsy, stroke, trauma, and neurodegenerative diseases. Moreover, apoptotic mechanisms are not just involved in apoptosis, but are also involved in the regulation of synaptic plasticity. It is not known, however, whether the balance between neuronal "birth" and "death" is impaired in the brain, particularly in the rostral ventrolateral medulla (RVLM), which determines sympathetic nerve activity. We examined the balance between neuroblasts, cell proliferation, and neural apoptosis in the RVLM of stroke-prone spontaneously hypertensive rats (SHRSP) in pre-hypertensive (6–8 weeks old) and hypertensive states (14–16 weeks old). **Method and results:** In SHRSP and age-matched Wistar-Kyoto (WKY) rats, we sampled the RVLM tissues by punched-out technique. We identified neuroblasts by staining for doublecortin (Dcx), cell proliferation by bromodeoxyuridine (BrdU), and neural apoptosis by staining for the active forms of caspase-3 and 9. In hypertensive states, SHRSP had significantly higher blood pressure than WKY, and significantly lower levels of Dcx and BrdU expression in the RVLM (evaluated by Western blot analysis) than WKY (Dcx; -43±4%, BrdU; -38±5%, n=5 for each, $P<0.01$). In pre-hypertensive states, the expressions of Dcx and BrdU in the RVLM were significantly decreased compared with WKY (Dcx; -33±5%, BrdU; -34±3%, n=4 for each, $P<0.01$), whereas blood pressure was similar between SHRSP and WKY. The expression levels of caspase-3 and 9 in the RVLM did not differ in SHRSP and WKY, in either pre-hypertensive or hypertensive states. **Conclusion:** The impaired neurogenesis, identified by the migration of neuroblasts and neural proliferation, in the RVLM might be involved in hypertension in SHRSP.

Lipoproteins

Subspecialty: Lipid Metabolism

Wednesday

West Hall A1-A2

Abstracts 1385–1393

1385

The ATP-binding Cassette A1 (ABCA1)-mediated Apolipoprotein A-I Lipidation Occurs at the Plasma Membrane and not in the Endocytic Compartments

Maxime Denis, Yves D Landry, Xiaohui Zha; Ottawa Health Rsch Institute, Ottawa, Canada

The ATP-binding Cassette Transporter A1 (ABCA1) is required for the biogenesis of HDL through the lipidation of lipid-poor apolipoprotein A-I (apoA-I). ApoA-I has been suggested to internalize with ABCA1, presumably to acquire lipids from the endosomal compartments, an important hub for cholesterol trafficking. The aim of our work is to determine how apoA-I get endocytosed and whether this internalization contributes to the biogenesis of HDL. When examined by confocal microscopy, we found that Cy3.5-apoA-I endocytosed rather slowly ($t_{1/2}$ = 15 min, in baby hamster kidney cells expressing ABCA1) and poorly co-localized with transferrin, consistent with a pathway independent of clathrin-coated pits. ApoA-I was instead found perfectly co-localized with FITC-dextran, a bulk phase uptake marker and, at later time points, with LysoTracker. This strongly indicates that majority of internalized apoA-I was delivered to the lysosomes. ABCA1 was not found to co-localize with endocytosed apoA-I. Similar observations were obtained in mouse macrophages and normal human fibroblasts. Next, in order to determine the functional significance of endocytosis to cholesterol efflux, we used sucrose or latrunculin A to inhibit apoA-I endocytosis. We show that apoA-I, transferrin and dextran uptake were abolished, but cholesterol efflux was not decreased. To specifically determine whether internalized apoA-I contributes to the biogenesis of HDL, we developed a method to strip off apoA-I from the cell surface. Our results show that internalized apoA-I do not significantly contribute to the biogenesis of HDL (< 20%). Together, our results suggest that the plasma membrane is the main platform where ABCA1-mediated lipidation of apoA-I occurs. Internalized apoA-I is mostly targeted for lysosomal degradation and therefore does not significantly contribute to the biogenesis of HDL.

1386

Inhibition Of Ceramide Biosynthesis Decreases Cardiomyopathy In Lipoprotein Lipase (LpL) Lipotoxicity

Tae-sik Park, Yunying Hu, Kazue Okajima, Columbia Univ, New York, NY; Jonathan Buchanan, Univ of Utah, Salt Lake City, UT; Shunichi Homma, Mercy M Davidson, Columbia Univ, New York, NY; E. Dale Abel, Univ of Utah, Salt Lake City, UT; Xian-Cheng Jiang, SUNY Downstate Med Cntr, Brooklyn, NY; Ira J Goldberg, Columbia Univ, New York, NY

Cardiac specific overexpression of glycosylphosphatidylinositol (GPI)-anchored human LpL ($hLpL^{GPI}$) leads to lipid-induced cardiomyopathy. Fatty acid (FA) oxidation was increased and glucose oxidation was decreased in isolated perfused $hLpL^{GPI}$ hearts. We hypothesized that excess FA uptake into the hearts increases ceramide and this alters glucose utilization and increases myocellular apoptosis, and causes dilated cardiomyopathy in $hLpL^{GPI}$ mice. To test